Welding of aluminum alloys to steels: an overview

M. Mazar Atabaki*, M. Nikodinovski, P. Chenier***, R. Kovacevic*[1]**

* Research Center for Advanced Manufacturing and Technology (RCAM), Southern Methodist University, Dallas, Texas 75205, USA

** U.S.A Army RDECOM-TARDEC, Warren, Michigan, USA

*** Onodi Tool & Engineering Co., Melvindale, Michigan, USA

Abstract

Since the need for the joining of dissimilar materials is increasing, a wide requirement of the numerous industries will lead to the development of joining techniques capable to join the elements from the miniature assemblies to extremely large earth-moving vehicles. Among the different materials, iron-based alloys and aluminum-based alloys are among the most significant materials that are finding applications on the various industries to offer more viable and sustainable products. However, welding of these metals has been always a kind of dilemma for the engineers. There are a certain number of methods to join these dissimilar metals but no one could establish a reliable or a sort of credible welding method for the industrial applications while quality, cost, human resources and facilities are taken into the main considerations. This paper reviews the recent welding methods for joining aluminum alloys to steels. The microstructural development, mechanical properties and application of the joints are discussed.

Keywords: Welding; Steel; Aluminum; Intermetallics

[1] Corresponding Author: Tel: +1 214 768 4865; Fax: +1 214 768 0812
E-mail: kovacevi@lyle.smu.edu (R. Kovacevic)

Report Documentation Page	*Form Approved* *OMB No. 0704-0188*

1. REPORT DATE	2. REPORT TYPE	3. DATES COVERED
01 AUG 2013	**Journal Article**	**07-03-2012 to 16-07-2013**

4. TITLE AND SUBTITLE
Welding of aluminum alloys to steels: an overview

5a. CONTRACT NUMBER
SP0700-99-D-0301

5b. GRANT NUMBER

5c. PROGRAM ELEMENT NUMBER

6. AUTHOR(S)
M Atabaki; M Nikodinovski; P Chenier; R Kovacevic

5d. PROJECT NUMBER

5e. TASK NUMBER

5f. WORK UNIT NUMBER

7. PERFORMING ORGANIZATION NAME(S) AND ADDRESS(ES)
Research Center for Advanced Manufacturing and Technology,Southern Methodist University,6425 Boaz Lane,Dallas,TX,75205

8. PERFORMING ORGANIZATION REPORT NUMBER
; #24148

9. SPONSORING/MONITORING AGENCY NAME(S) AND ADDRESS(ES)
U.S. Army TARDEC, 6501 East Eleven Mile Rd, Warren, Mi, 48397-5000

10. SPONSOR/MONITOR'S ACRONYM(S)
TARDEC

11. SPONSOR/MONITOR'S REPORT NUMBER(S)
#24148

12. DISTRIBUTION/AVAILABILITY STATEMENT
Approved for public release; distribution unlimited

13. SUPPLEMENTARY NOTES

14. ABSTRACT
Since the need for the joining of dissimilar materials is increasing, a wide requirement of the numerous industries will lead to the development of joining techniques capable to join the elements from the miniature assemblies to extremely large earth-moving vehicles. Among the different materials, iron-based alloys and aluminum-based alloys are among the most significant materials that are finding applications on the various industries to offer more viable and sustainable products. However, welding of these metals has been always a kind of dilemma for the engineers. There are a certain number of methods to join these dissimilar metals but no one could establish a reliable or a sort of credible welding method for the industrial applications while quality, cost, human resources and facilities are taken into the main considerations. This paper reviews the recent welding methods for joining aluminum alloys to steels. The microstructural development, mechanical properties and application of the joints are discussed.

15. SUBJECT TERMS
Welding; Steel; Aluminum; Intermetallics

16. SECURITY CLASSIFICATION OF:			17. LIMITATION OF ABSTRACT	18. NUMBER OF PAGES	19a. NAME OF RESPONSIBLE PERSON
a. REPORT	b. ABSTRACT	c. THIS PAGE			
unclassified	**unclassified**	**unclassified**	**Public Release**	**43**	

Standard Form 298 (Rev. 8-98)
Prescribed by ANSI Std Z39-18

1. Introduction

As many of the metals, ceramics and compounds can be joined together there are still many unsolved problems in the joining of different alloys and compounds which basically is emanated from the different thermal, mechanical and structural properties. On the other hand, there is certainly an increasing trend towards the use of dissimilar joints in the gigantic industries including shipbuilding, military vehicles, aerospace and automobile industries.

The sound joint is the highest concern through the design of the parts especially for such places where the quality of the joints has more priority than other concerns. Most of the thinking about the new replacement of the light materials is that it will help to reduce the fuel consumption, cost of the production and effectively reduces the amount of human-elemental energies on the heavier materials. For instance, the use of the aluminum alloys and steels and finding the surrogating material for some of the sensitive components is relatively influenced by the controlling forces like current regulations to encounter fuel efficiency standards by decreasing vehicle weight, and to meet recycling standards [1, 2]. The result of this shift is to provide new technologies to join the materials together as some components still need to be made of hard and toughened steels. There are, however, numbers of works on the application of different welding technologies to bond these interesting alloys but the problem of losing the strength in the bond areas is always a big challenge which up to now, because of the formation of the brittle intermetallics, has not been solved [3,4]. Except the above mentioned problem large electrochemical difference of 1.22 volts, subsidiary precipitates created during solidification, different thermal properties, dissimilar thermal expansion, heat capacity and thermal conductivity, lattice transformation, large difference between the melting points (660 °C for Al alloy and 1497 °C for steel) and nearly zero solid solubility of iron in aluminum are creating the large discrepancy between the metals causing distortion, formation of the cavities and cracks, leading to the reduction of the mechanical properties after the joining processes. Laser roll bonding [5], impact welding [6], friction welding [7], ultrasonic welding [8], diffusion bonding [9], explosive welding [10], friction stir welding [11], laser brazing/welding [12, 13], magnetic pulse welding [14] and laser pulse welding [15, 16] are the typical welding processes that have been applied up to now to join different grades of the steels to the aluminum alloys. However,

the key point in the development of a novel technique to join the alloys is a way to control the size and quantity of the Al/Fe intermetallic layer by controlling the heat sink or seizing the formation of the intermetallics by using the transition inserts or brazing the steel to other compatible materials and then join it to the aluminum alloy.

In the present review, current application of the joining techniques for making stronger bonds of aluminum alloys and different classes of steels are presented. However, the most recent research works on the investigation of the bonds are reviewed. The current ideas, models and simulations on these joints, examined in different welding techniques, are also illustrated in details with the hope that it helps the engineers to come up with new ideas, resolutions and above all cost effective joining techniques for the dissimilar materials.

2. Recent technologies for joining aluminum alloys to steels

Before exploring any of the bonding processes it might be better to explain a little bit about the techniques that have been applied so far to join the metals together and then have an overview of the physical phenomenon during the fusion and solid state welding of the aluminum alloys to steels. As the welding processes are fundamentally categorized into two main streams, fusion and solid state, there are physical, chemical, mechanical and even statistical analyses to explain the reactions during the bonding of the materials. In the fusion bonding of the metals the heat source generates a temperature field which is very inhomogeneous and varies over time. Thermal variation occurs in the regions of the heat source and its adjacent areas. The microstructural variations in the fusion zone, deformed area and heat affected zone dominate the changes in the total behavior of the bonds as a result of non-uniform heating and solidification. Extreme crack propagation, intermetallic formation, porosity and other imperfections arise in connection with the typically inhomogenous phase changes and solidification. Considerable residual stresses, weld shrinkage, welding distortion and deformations are a few examples of the unwanted consequences which somehow would lead to brittle fracture, fatigue fracture, shape instability and stress corrosion cracking. As the formation of Fe_xAl_y phases are necessarily

irresistible an excessive formation of the intermetallics lead to the brittleness of the bonds (Fig.1).

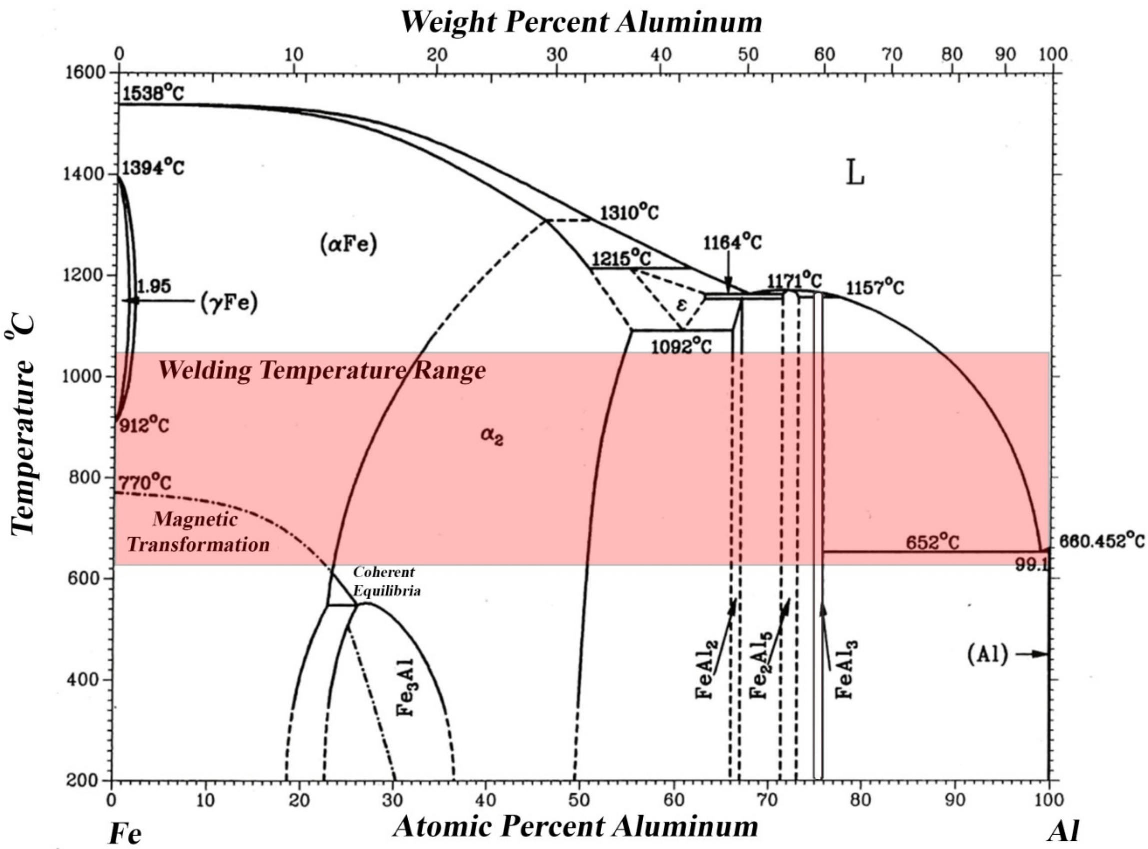

Fig.1. The dual phase diagram of the Fe-Al [improved version of 3].

In the atomic scale the atoms of the aluminum alloys and steels can be moved during the bonding processes as a function of the number of vacancies, diffusion of small solute like carbon and hydrogen which is called interstitial diffusion and grain boundary moving. The equilibrium phase diagram shows seven non-stoichiometric intermetallics (Fe_3Al, FeAl (α_2), $FeAl_2$, Fe_2Al_3 (ε), Fe_2Al_5 and FeA_{l3}, $FeAl_6$). Table 1 designates the most important characters of theses intermetallics.

Table 1. Stability range, crystal structure and hardness of the intermetallics [17- 19].

Phase	Stability range (*at.*%)	Crystal structure	Vickers Hardness	Activation Energy (*eV*)	Density (*g/cm*^{3})
Fe solid solution	0-45	BCC	-	-	-
γ-Fe	0-1.3	FCC	-	-	-
FeAl	23-55	BCC	470-667	2.1	5.37
Fe_3Al	23-34	Ordered BCC	330-368	-	6.67
Fe_2Al_3	58-65	Complex Cubic	-	-	-
$FeAl_2$	66-66.9	Triclinic	1058-1070	-	4.36
Fe_2Al_5	70-73	BCC Orthorhombic	1000-1158	1.5	4.11
$FeAl_3$	74.5-76.5	Highly complex Monoclinic BCC	772-1017	-	3.95
$FeAl_6$	-	-	-	1.2	-
Al solid solution	99.998-100	FCC	-	-	-

However, the enthalpy of the formation of the intermetallics can be calculated by the following equation [20].

$$\Delta H = X_{Al}\Delta H_{Al}^{ef} + X_{Fe}\Delta H_{Fe}^{ef} - \Delta H_{Al_{x_{Al}}Fe_{x_{Fe}}}^{ef} \quad (1)$$

where X_{Al} and X_{Fe}, are mole fractions of the Al and Fe, ΔH the formation enthalpy of the intermetallic at the room temperature, ΔH_{Al}^{ef}, ΔH_{Fe}^{ef} are dissolution heat effects of one mole

atoms of Al and Fe in the solvent and $\Delta H^{ef}_{Al_{x_{Al}}Fe_{x_{Fe}}}$ is the heat effect accompanying the dissolution of one gram-atom of the intermetallic. The probable thermodynamic reactions between the aluminum and steel can be presented by the Scheil's relations as it is shown in Fig.2.

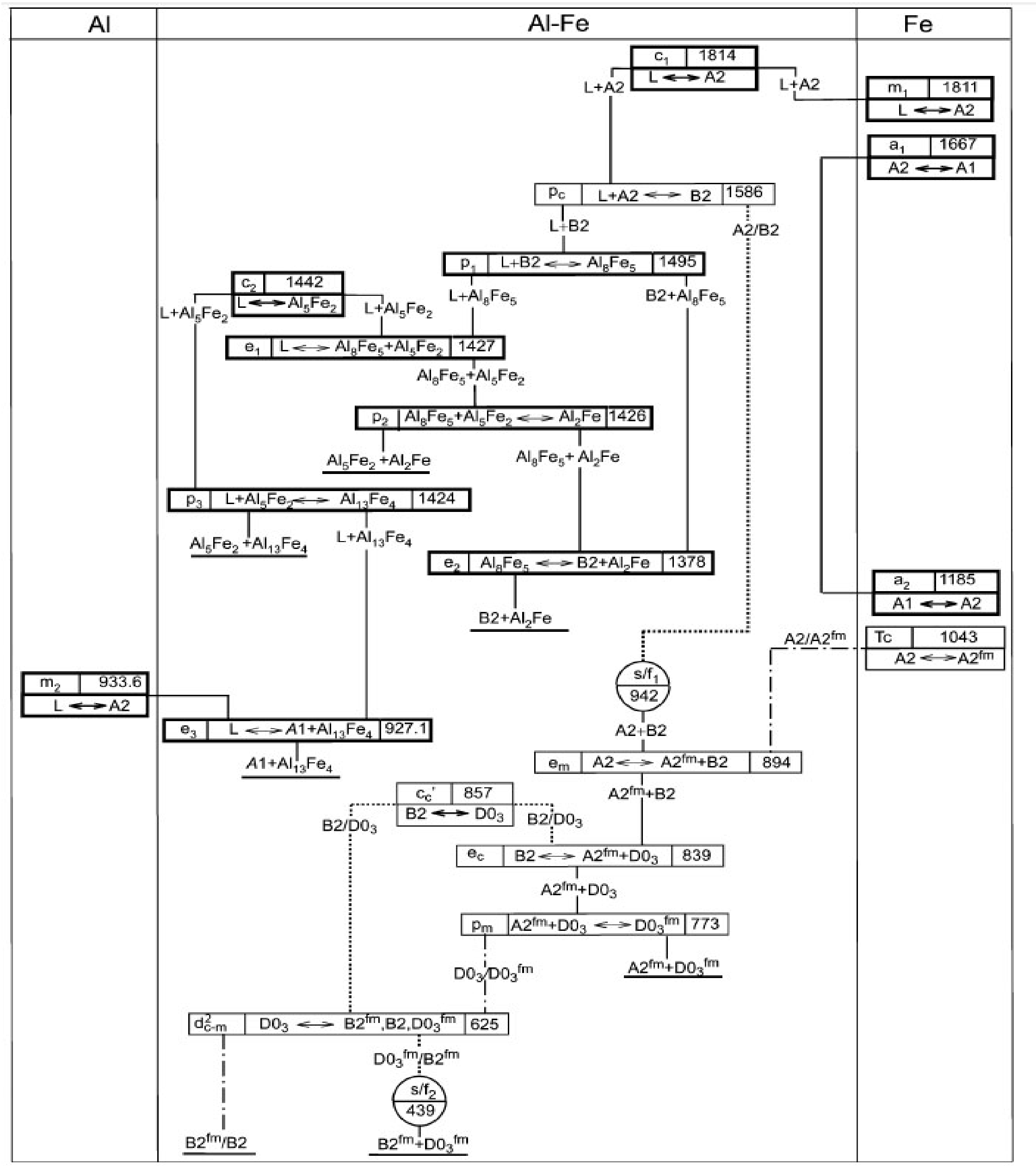

Fig.2. The calculated possible reactions between aluminum and iron during the cooling [21].

2.1. Fusion welding methods

2.1.1. Gas metal arc (MIG) welding and tungsten inert gas (TIG) welding techniques

One of the aluminum alloys named 2B50 and stainless steel (1Cr18Ni9Ti) were welded by MIG welding using Al-Si filler metal (4043). The influence of the aluminizing coating and galvanized zinc coating on the fusion metal spread-ability was studied [22]. The results showed that the aluminized coating had imperfect influence to improve the appearance of the weld bead and there were many micro-cracks in the middle of the bond zone. The fracture, as a result, mostly happened at the interfacial layer of the weld showing just 60 MPa ultimate strength. The study indicates that the intermetallic compound ($Al_{4.5}FeSi$) can be formed in the fusion zone near the interface of the weld zone and heat affected area. The thickness of the intermetallic compound layer was measured to be around 5 μm to 15 μm for the heat input of 0.846 KJ/cm [22]. In another research the aluminum alloy was joined to the stainless steel by the MIG welding and the intermetallic layer with a thickness of greater than 40 μm was achieved [23]. In another study, a thin aluminum alloy sheet (5A02) was welded to stainless steel 304 using a flux-cored Zn-15%Al alloy wire. It was shown that annealing at 280 °C for 30 min after the welding can enhance the strength of the bond. The thickness of the intermetallic layers was reported to be about 1.5 μm while ZnO was formed in the weld areas. Other kinds of intermetallics were also detected close to the stainless steel side [24, 25]. However, the grains could be refined about 27% during the gas tungsten arc welding of the materials by the ultrasonic technique and post weld heat treatment at 280 °C might lead to increasing the bond strength two times more [26].

Tungsten inert gas welding of an aluminum alloy (5A06) to austenitic stainless steel was performed applying aluminum-based filler metal and non-corrosive flux (see Fig.3). The results indicated the formation of different brittle intermetallics with the thickness range of 5 μm to 35 μm [27]. The different phases detected were τ_5-$Al_{7.2}Fe_2Si$, η-Fe_2Al_5 and $FeSi_2$, giving an average tensile strength of 140.0 MPa and having the fracture occurred in the filler alloy, at the corner of the bond area. The formation of these phases can be predicted by the ternary phase diagrams and if the right path has been chosen the nucleation of these kinds of phases can be prevented (see Fig.4).

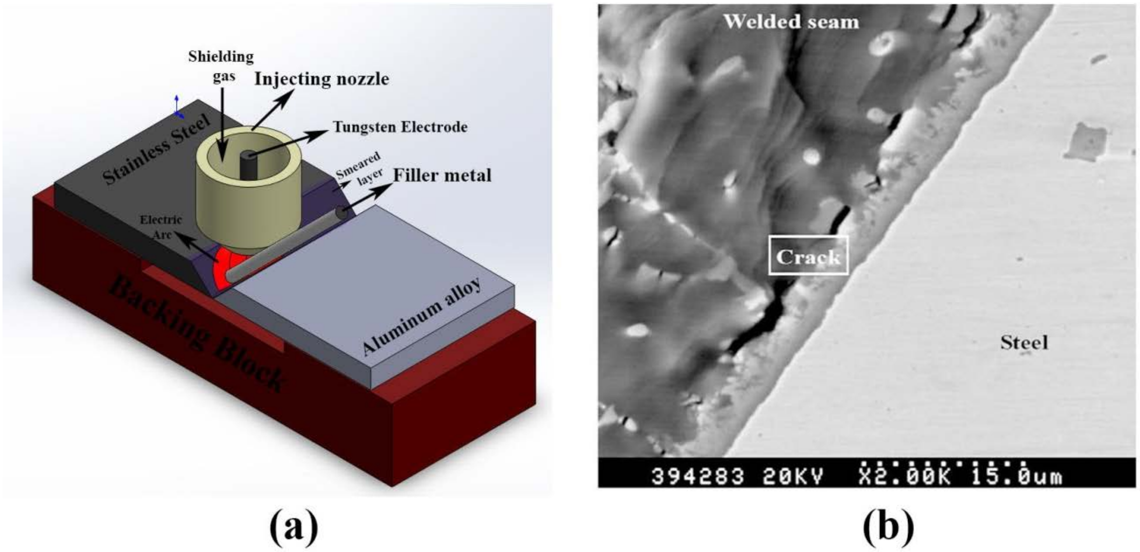

Fig.3. (a) Schematic of the butt TIG welding for joining the aluminum to steel and (b) formation of the cracks at the interface [27, 28].

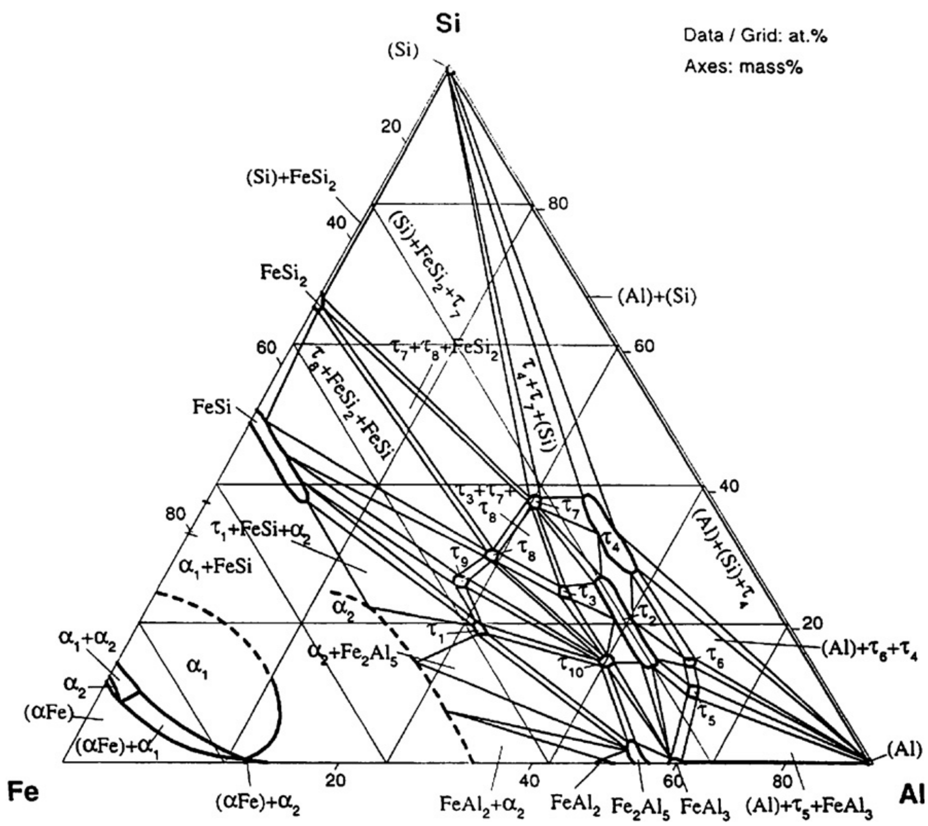

Fig.4. Ternary phase diagram of the Al-Fe-Si system at 600 °C [27].

An aluminum alloy and galvanized steel were welded by a cold metal transfer joining method [4]. A pure aluminum (99.8 % Wt.) was used for that study and it was shown that the thickness of the intermetallics, mainly trapezoidal equiaxial Fe_2Al_5 and elliptical $FeAl_3$, could be reached to 2.3 μm. The scanning transmission electron microscopy (STEM) micrograph of this study shows microtwins and Grisslile dislocations within the intermetallics as shown in Fig.5. The $FeAl_3$ was said to be a kind of monoclinic phase with the lattice constants of α=1.5489 nm, b=0.8083 nm, c=1.2476 nm, β=107.70 °. An alternative gas metal arc welding process, alternate-current double-pulse gas metal arc welding, has been proposed for joining a thin aluminum alloy (5052) to galvanized mild steel in the lap-joint configuration with the help of a filler wire (4047) [29]. Besides of the novel idea, the bonds weakened because of the nucleation and growth of Fe_2Al_5, $FeAl_3$ and Fe_3Al.

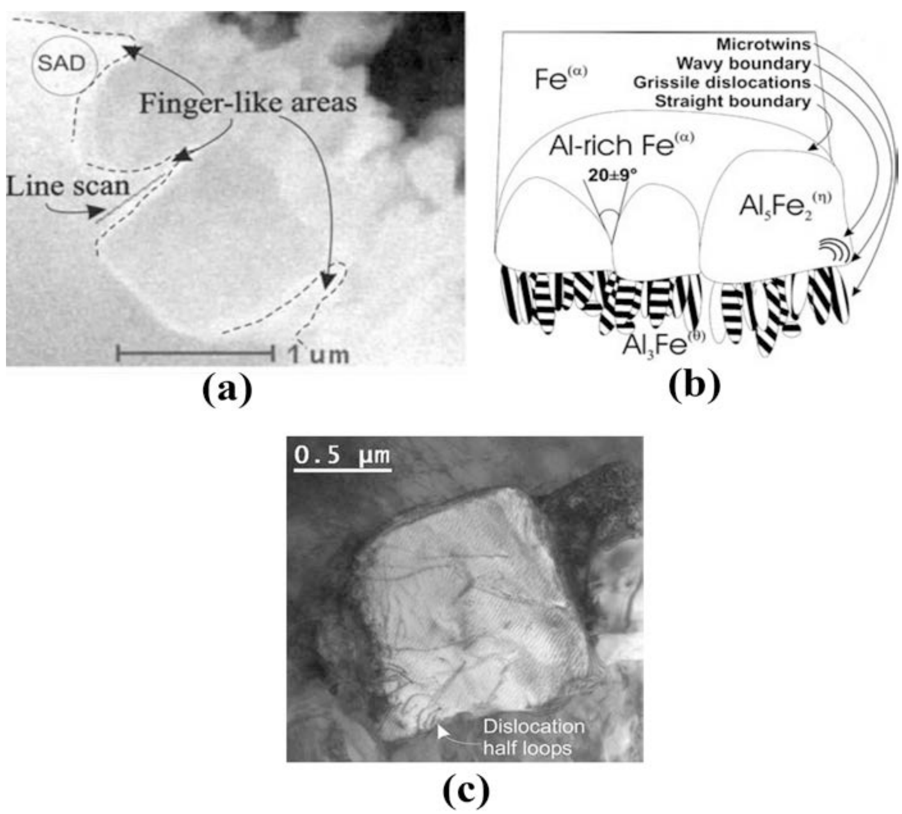

Fig.5. (a) STEM micrograph of the finger-like intermetallics, (b) schematic of all the phases and their defects and (c) bright field TEM micrograph of an Al_5Fe_2 showing Glissile dislocation half-loops [4].

The cold metal transfer welding of thin aluminum alloy bonded to a mild steel (Q235) by the help of aluminum filler metal (Al4043), was proposed as a prospect on the application of this technique to reduce the thickness of the intermetallics [30].

2.2.2. Resistance spot welding

There are some reports on the joining of the steels to aluminum alloys by the resistance spot welding. In one of the researches, the welding current during the bonding process was altered every 1 kA between 5 kA and 12 kA at the welding time of 0.2 s and an electrode force of 2 kN. The schematic of the resistance spot welding is presented in Fig.6. The thickness of the reaction layer was thin at the peripheral region and it was thicker in the middle of the bond area. The fracture crack was significantly propagated through the aluminum alloy (A5052) in the peripheral region of the weld and through the reaction layer in the central region of the weld, from an intermetallic layer with the thickness of about 1.5 μm [31, 32]. A comparison was made for the reaction layers formed at the A5052/SUS304 interface and A5052/SPCC interface indicating the reaction layer at the interface of the A5052/SUS304 was thinner than the one formed for the A5052/ Steel plate cold commercial (SPCC).

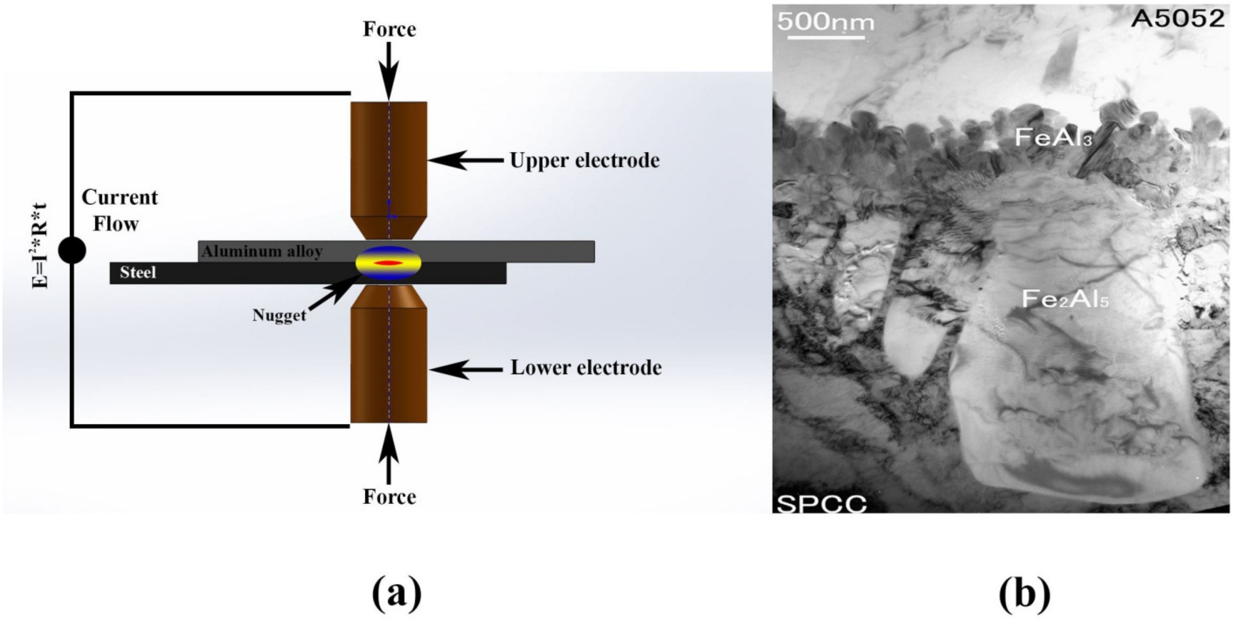

Fig.6. (a) Schematic of the resistance spot welding for joining the aluminum alloy (A5052) and stainless steel (Steel plate cold commercial (SPCC)) and (b) bright field image of the interface showing $FeAl_3$ and Fe_2Al_5 formed at the interface [32].

It was shown that there is a relationship between the welding current and the nugget diameters during the resistance spot welding of the A5052/SPCC and A5052/SUS304 bonds. The nugget diameter was increased with the enhancing the welding current. Under the same spot welding current, the nugget of A5052/SPCC bonds presented nearly the equal diameter, while the A5052/SUS304 bonds exposed larger nugget diameter because of the poorer electrical conductivity and specific heat of the SUS304 [33, 34].

In another work, in order to overcome the problems associated with the direct resistance spot bonding of the aluminum alloys to steels a transition layer was introduced as a compatible material to both sides of the bond zone [35]. The interlayer was cold-rolled to the aluminum side and then the bond was made under the copper tips of the spot welding machine. The fatigue results showed higher fatigue strength of the joints with transition layer than that of purely spot welded coupons. The work extended by applying the finite element method to explore the effect of the transition material on the bond quality [36]. It was shown that the nugget on the steel side

has a regular and elliptical shape with dendritic grain structure while the side of aluminum showed a top-cap ellipsoidal structure with the formation of pores and cavities inside the cap. This finite element analysis suggested the heat for the nugget formation on the aluminum side was vastly conducted from the steel side.

2.2.3. Laser welding and electron beam welding

A type of low carbon steel (structural steel) was laser welded to an aluminum alloy (5754) in the keyhole welding mode with the overlap configuration. For reducing the formation of intermetallics during the bonding process the effect of laser power, pulse duration and overlapping factor were studied. With enhanced laser power, pulse duration and overlapping factor the amount of intermetallic components inside the weld region was increased whereas decreasing the main parameters produced inadequate penetration depth and cavity (Fig.7). It was indicated that the appropriate tensile strength can be achieved when the amount of the intermetallics is reduced to the lowest possible amount [15]. It was believed that when the penetration depth is limited between 1560 and 1630 μm, an appropriate surface quality and lower amount of intermetallics can be created. In this investigation the amount of the intermetallics was measured by the following relationship:

$$I_{Total} = \frac{A}{A'} \times 100 \quad (2)$$

where I_{Total} was the total amount of the intermetallics, A the area of intermetallic components and A' was the area of the weld zone.

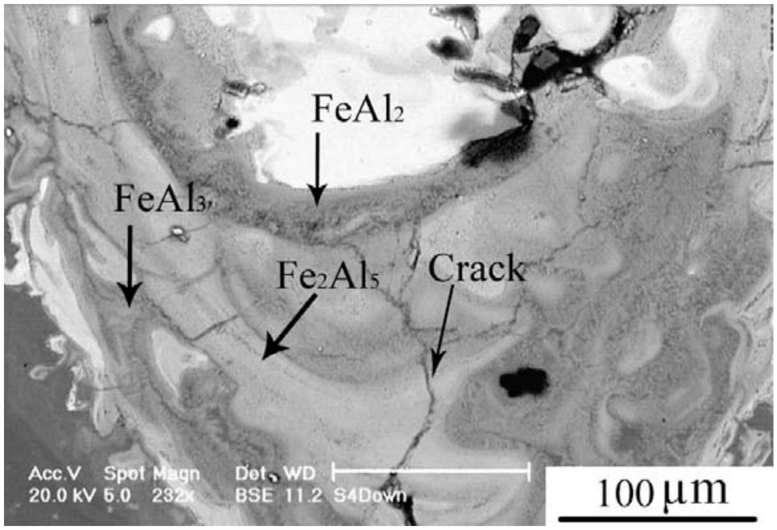

Fig.7. SEM micrograph of the bond shows $FeAl_3$, Fe_2Al_5 and pores [15].

The laser brazing was a solution proposed by some of the references. It allows having a localized fusion of the materials ensuing in the control of the growth of the intermetallics. For example, a filler wire composed of 85% Zn and 15% Al was used to join the aluminum to steel and the process has been optimized by the Taguchi Method [37]. The tensile strength of about 200 *MPa* was reported while a significant fracture was seen in the heat-affected zone [38, 39]. The thickness of intermetallics was within the range of 3-23 μm. In another work [40], the steel (JSC270CC) and aluminum alloy (A6111-T4) was welded by the dual-beam YAG laser with the continuous wave and pulse wave modes. Formation of a 10 mm thick semi-circular intermetallic layer at the bottom of the weld zone and shearing strength of 128 MPa were reported. Conduction mode laser welding of a thin galvanized steel and an aluminum alloy (AA5083-H22) also confirm the formation of $FeAl_3$ and Fe_2Al_5 [41].

A defocused laser beam was used to join aluminum alloy (A6111) and low-carbon steel (SPCC) in a lap-joint configuration. It was reported that since the depth of the molten pool in the steel side kept about 90% of the steel thickness, the area near the upper surface of the aluminum could be melted with the semi-elliptical shape [42, 43]. However, the maximum shear strength of the lap joint was around 70 % of the A6111-T4 and needle-shape intermetallics were formed in

the molten pool confirming the presence of $Al_{13}Fe_4$, Al_5Fe_2, Al_2Fe, FeAl, Fe_3Al and Al_6Fe (Fig.8).

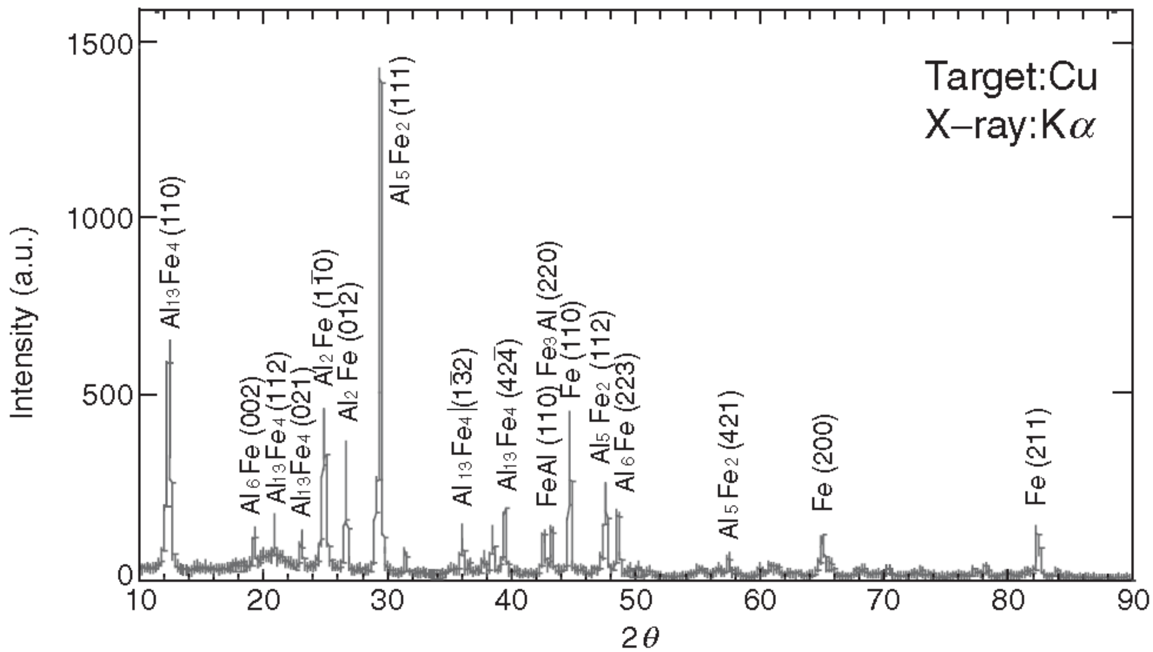

Fig.8. X-ray diffraction pattern shows the presence of different kinds of intermetallics on the fracture surface of the coupons [42].

The other alloy from the aluminum alloy series (AA6016) was laser brazed to low-carbon galvanized steel with different thicknesses, by a zinc-based aluminum filler alloy. The work shows that $Fe_2A_{l5}Zn_x$ type intermetallics with 10-µm thickness can be formed in the bond area [44]. In an interesting research [45], a 10 kW fiber laser with a tightly focused spot diameter of 200 µm was employed to join a stainless steel (304) and an aluminum alloy (A5052), separately. The study was given an indication of the influence of the laser beam based on a high speed charge-coupled device (CCD) camera which was partially exposed out of the keyhole region at a certain speed. The weldability of aluminum (AA 1100) and stainless steel (AISI 409) by the pulsed Nd:YAG laser welding process was studied and the influence of the pulse time and power density on weld diameter, penetration, bond area and porosity was qualitatively explained concerning material-dependent variables such as the thermophysical properties of the parent

alloys [46]. The power density required for melting the aluminum was reported to be almost 4.5 times higher than the stainless steel. Galvanized steel was joined by the laser brazing to the aluminum alloy (4043) using a fiber laser in the keyhole mode and the presence of α (τ_5)-Al_8Fe_2Si, θ-$Al_{13}Fe_4$ and ζ-Al_2Fe, causing the maximum strength of 162 MPa and brittle fracture was reported [47]. Some of the specific joint shapes essentially needed a design for the filler alloy, filling the gap between the two components. Two different galvanized steel flanges were laser brazed using a zinc-based filler wire with Nd-YAG laser where the formation of different intermetallics was recorded [48]. The interesting point in the research was the suggestion on the use of a pre-heat source as the second one like laser towards the steel side during the bonding. The other recommendation which might affect the dimension and geometry of the intermetallics is a method to sink the heat out of the bond area in order to reduce the heat input within the molten pool. Copper backing blocks are very familiar in the welding industry and their use was studied to control the heat flow with the successful report on the reduction of the intermetallic layers during the laser welding of a high strength steel (Dual-TEN 590 steel) and A6022-O aluminum alloy [49].

Furthermore, the influence of the penetration depth in the key-hole mode of the laser welding of aluminum alloys (6016, 6056 and 6061-T6) to a low carbon steel (DC 04) showed that the presence of $FeAl_3$ and Fe_2Al_5 with the 20 μm and 5 μm is a kind of irresistible response to the fusion laser welding process [13,50]. However, the medium penetration through the steel provides interlocking behavior of the joints giving a little bit higher strength, since the aluminum was at the top [13]. Application of bimetals for the laser welding process was another solution presented by Liedl *et al.* [51] in which the bimetal wires can be roll welded Al/Steel strips and the welding is a kind of tricky process to have similar metals joined together. There, correspondingly, might be a correlation between the optical emission of the plasma and the vapored materials which can be predicted by the spectroscopy technique.

Electron beam welding was another method to bond aluminum alloy and steel while a silver interlayer was used in the sandwiched coupons. The joint was full of Ag_2Al intermetallic which its amount was highly dependent on the electron beam power and beam offset [52]. When

the beam offset was large enough two other intermetallics namely FeAl and $FeAl_3$ were formed. However, the bonds were weaker than the both parent metals.

2.2. Solid state welding methods

2.2.1. Ultrasonic welding

The aluminum and steel can be welded by a 15 kHz ultrasonic butt welding system with a vibration source applying eight bolt-clamped Langevin type PZT transducers and a 50 kW static induction thyristor power amplifier [8]. It was shown that the large vibration amplitude of 25 µm, static pressure of 70 MPa and welding time of 1.0-3.0 s can produce a reasonable high strength joint (Fig.9).

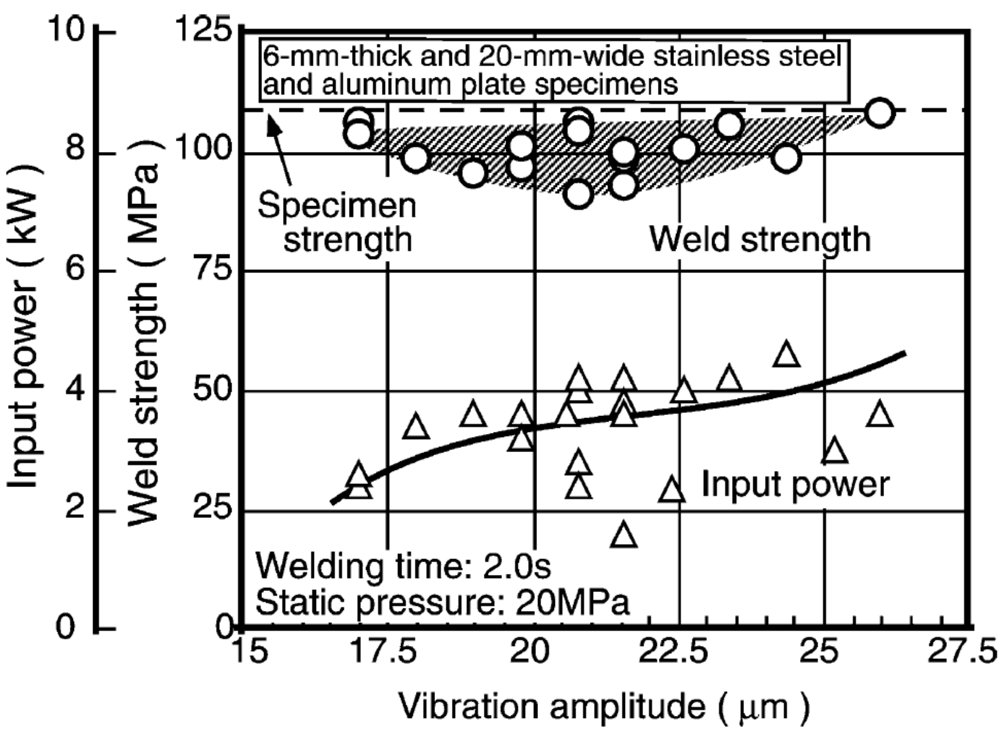

Fig.9. The relationship between vibration amplitude, input power and weld strength of joint between the pure aluminum and electrolytically polished stainless steel [8].

2.2.2. Magnetic pulse welding

Some of the aluminum alloys (A1050, A2017, A3004, A5182, A5052, A6016, and A7075) were joined to the steel (SPCC) by the magnetic pulse welding [14]. The breakthrough in the study was the design of the coil which was an E-shaped flat coil (Fig.10).

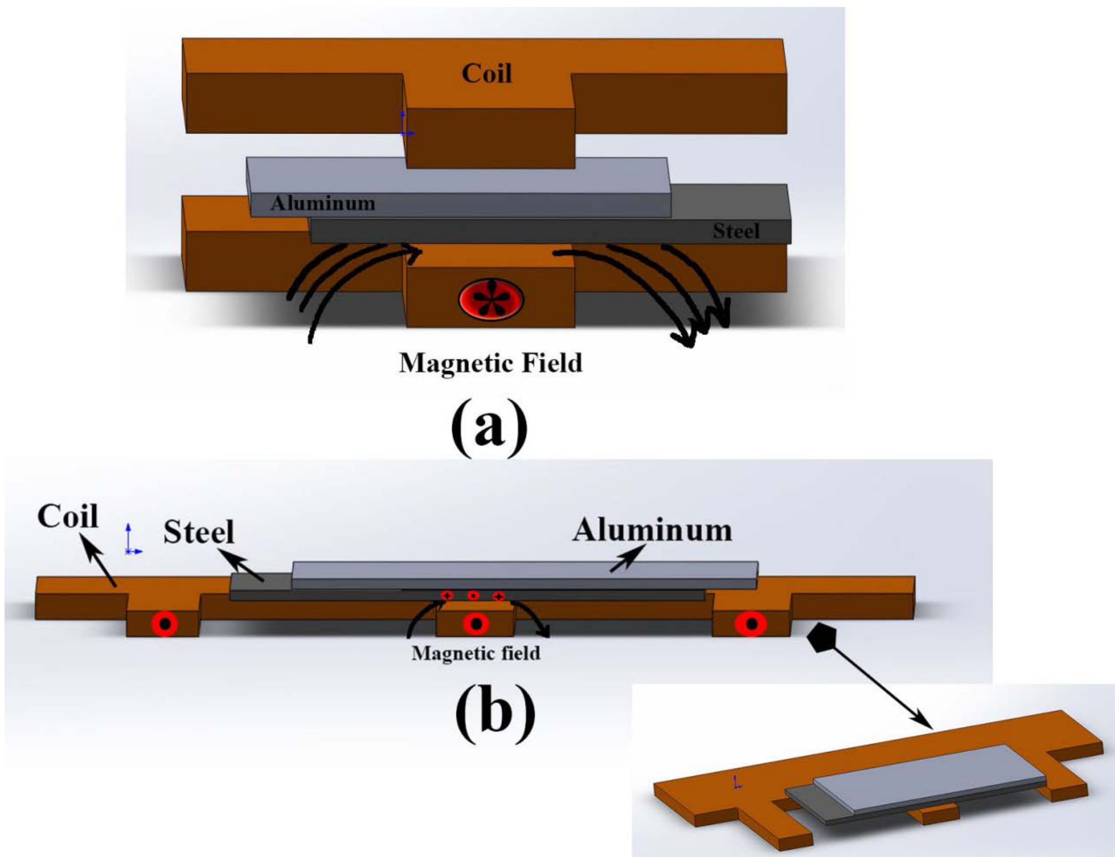

Fig.10. The coil designs for the magnetic pulse welding (a) T-shape and (b) E-shape [14].

The eddy current i and the magnetic pressure p can be given as [14]:

$$\nabla \times i = k\left(\frac{\partial B}{\partial t}\right) \tag{3}$$

$$p = \left[\frac{\left(B_0^2 - B_i^2\right)}{2\mu} \right] = \left(\frac{B_0^2}{2\mu} \right)(1 - \exp(\frac{-2x}{\delta})) \quad (4)$$

where κ, μ, τ, B_o, and B_i are the electrical conductivity, magnetic permeability, thickness, and magnetic flux density for the lower and upper surface dissimilar sheet, respectively. The depth of skin effect can be obtained by $\delta = \sqrt{(2/\omega\kappa\mu)}$, where ω is the angular frequency of changing field [14]. A kind of wave morphology and the intermediate layer was observed along the bond interface. Additionally, grain refinement in the A6111 matrix near the weld interface has been recorded [53]. High shear strength was reported because of the greater penetration of the magnetic field in the center of the bond area but the edges of the bonds show the weakness of the prepared bonds [54].

2.2.3. Roll bonding

A steel alloy (stw22) was welded to an aluminum alloy (Al1350) at different pre-heat temperatures and thickness reductions by the roll bonding [55]. After using the peeling test the study showed that the brittle surface between the aluminum and steel was the main cause of the failure. It was shown that the main parameters controlling the bond behavior are the rolling speed, preheating and roll-strip frictional condition [56-59].

2.2.4. Diffusion bonding

In one of the studies [60], diffusion bonding was applied to join an austenitic stainless steel (316) to two different aluminum alloys (1100 and 6061), using silver interlayer coated on the surface of the parent metals by a hot hollow cathode faying surface coating technique and then the joints were aged at different temperatures. There was a huge vicissitude in the reported mechanical properties emanating from the initiation and growth of intermetallics between three different alloys. The microscopic analysis showed the formation of Ag_2Al and Ag_3Al at the

faying surface of the aluminum alloy. It was shown that the coupons aged at 423 K gives lower development of the intermetallic with respect to the time of the aging (see Fig.11).

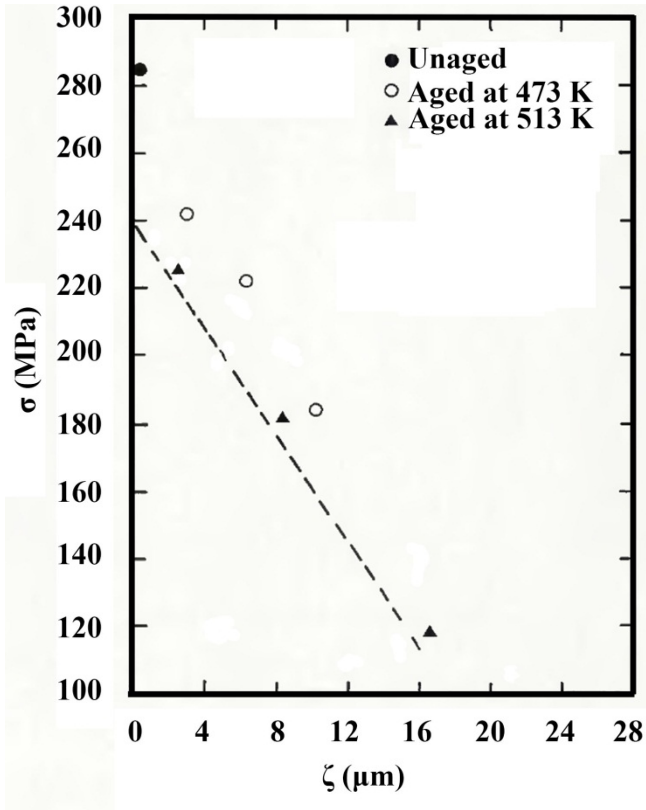

Fig.11. The dependency of the strength of the bonds prepared by the diffusion welding between stainless steel (304) and aluminum alloy (1100) on the total thickness of the intermetallic layer [60].

In the other investigation, a different aluminum alloys (Al 1060) and steel (1Cr18Ni9Ti) were joined together using the vacuum furnace and A-Si alloy as the strip layer. The interface of the joints showed the vast formation of δ (Al, Fe, Si) and α-Al (Si), with reportedly less brittleness of the interaface [61]. It was found that during the diffusion bonding at 873 K causes the formation of $FeSiAl_5$, $FeAl_3$ and Fe_3Al intermetallics [62-66]. The mass balance equation at the boundary between Fe_3Al and $FeAl_3$ can be said to have the following form [67]:

$$(C_1 - C_2)\frac{d\xi}{dt} = -D_1(\frac{\partial C}{\partial x})_{C_1} + D_2(\frac{\partial C}{\partial x})_{C_2} \quad (5)$$

where D_1 is the diffusion coefficient of Fe in Fe_3Al and D_2 is the diffusion coefficient of Fe in $FeAl_3$. The diffusion of the aluminum to the steel can be estimated by the Boltzmann solution of Fick's second law [68, 69]:

$$D_S = \frac{1}{2t_b}\frac{\partial x}{\partial C_S}\int_{C_{S_1}}^{C_S} x dC_S \quad (6)$$

where x is the position of the solute, t_b is the diffusion brazing time, and C_S is the concentration of the solute in the steel. It was recommended that the development of the intermetallics is a diffusion-controlled process since the thickness of the layers proved a linear link to the square root of the diffusion time [70]. Therefore, the growth of the intermetallic layer (Y) can be explained by:

$$Y_{FeAl} = 5.74\times10^3 t^{0.5}\exp(-\frac{9\times10^4}{RT}) \quad (7)$$

$$Y_{Fe_3Al} = 2.75\times10^5 t^{0.5}\exp(-\frac{1.39\times10^5}{RT}) \quad (8)$$

where K_0 and K are constant, R is the gas constant, Q is the activation energy for growth of the intermetallic and T is the process temperature. The activation energies for the growth of the FeAl and Fe_3Al intermetallics were alleged to be 180 and 260 kJ mol^{-1}, respectively [71]. It was suggested that the development of the Fe_2Al_5 was mainly controlled by the diffusion interaction and follows a parabolic law, whereas the development of $FeAl_3$ is completely linear and controlled by the reaction on the interface [71, 72]. However, the growth rates and activation energies of the Fe_2Al_5 and $FeAl_3$ were reduced by the increase in the amount of Si in the aluminum alloy. Fig.12 shows the electron backscatter diffraction inverse pole figure maps of the different intermetallic layers between steel and aluminum alloys. It was demonstrated that the reaction of the steel with Al-5 wt.% Si at 600 °C lead to thicker reaction layers in comparison to the reaction of the steel with pure aluminum [72].

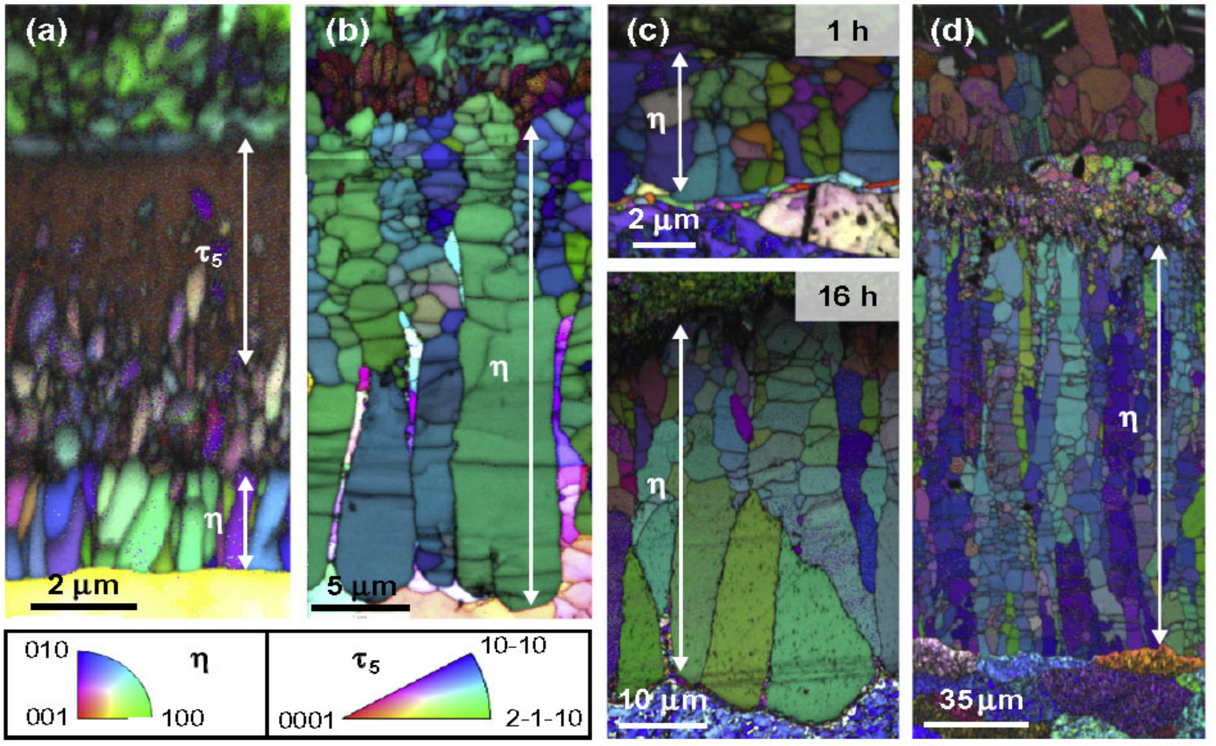

Fig.12. Electron backscatter diffraction inverse pole figure maps for different reaction layers between steel and aluminum alloys: (a) the interdiffusion at 675 °C for 30 s for the Al-5 wt.% Si/steel, (b) the interdiffusion at 675 °C for 30 s for pure aluminum/steel, (c) the interdiffusion at 600 °C for 1 h (top) and 16 h (bottom) for pure aluminum/steel and (d) the interdiffusion at 600 °C for 16 h for Al-5 Wt.% Si/steel [72].

In the tensile test experiment, it was shown that the interfacial failure mostly occurred for the pure aluminum/steel joints with the intemetallic layer thickness of 7 μm. The failure in the Al-5 Wt.% Si/steel joints occurred within the η phase with the thickness of 1.6 μm [73]. Direct bonding of pure aluminum (in a cubic form) and stainless steel 304 and 316 (in a cylindrical shape) was performed, without heating, in an ultra-high vacuum since the preparation of the specimens was a kind of troublesome process by activating the surface using argon fast atom beam for long hours min under the pressure of 6.0×10^{-5} Pa followed by close contact under an external pressure of 960 N [74]. The maximum tensile strength of 100 Mpa reported for this technique.

2.2.4. Explosive welding

Bimetals were fabricated from a high strength low alloy steel (1.45 Wt.% Mn-0.2 Wt.% Si-0.186 Wt.%) and dual phase steel joined to the aluminum alloy, separately by the explosive welding and the shear strengths of 420 MPa and 720 MPa were reported, respectively (Fig.13) [75]. An aluminum alloy (AA5083) and a steel (SS41) were explosively-clad while an aluminum alloy (AA1050) was at the interface of the specimens [76]. It was demonstrated that the bond zone was composed of $FeAl_3$.

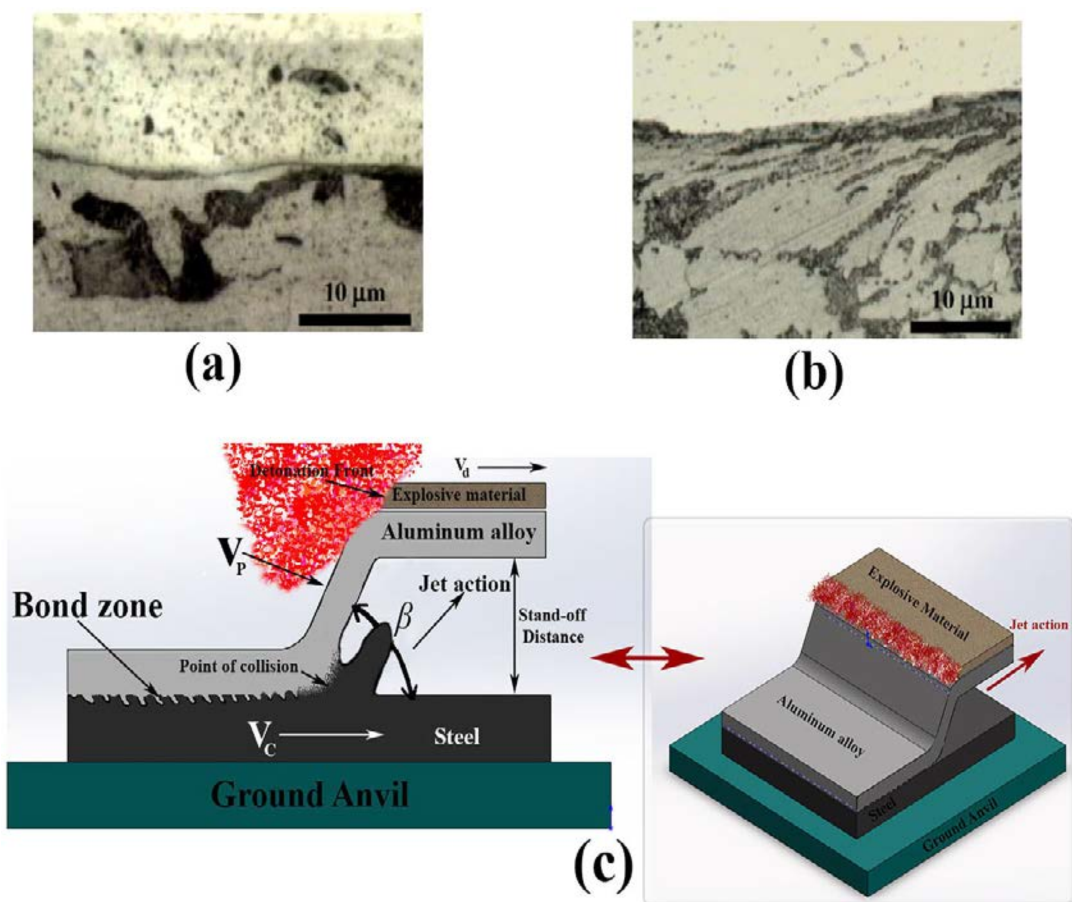

Fig.13. The microstructures of explosively welded: (a) high strength low alloy steel to aluminum and (b) aluminum to dual phase steel and (c) schematic of the bonding process [10].

The bonding interface of explosively-welded aluminum and steel with three different explosive materials was investigated showed that the waves with curled front were formed by the superplastic deformation and presence of AlFe, Al_2Fe, Al_3Fe and Al_6Fe intermetallics [77]. The corrosion test of the explosively welded aluminum to steel in the fast flow of sea water displayed substantial galvanic corrosion [78]. The structural transitions made of more materials by the explosive welding are one of the prospect technologies that should be more developed. There is a lack of enough theoretical and scientific investigations on these joints but in one of few studies the interfacial toughness of the aluminum and steel joints was studied by the compact tensile test and four points bending test, showing that the bonds should not exceed 400 °C during the welding process [79]. A triple cladding layer made of steel (A516)/pure aluminum (AA1050)/aluminum alloy (AA5083) which was explosive welded was heat treated and the effect of the heating on the shear stress of the bonds declined by increasing the time and temperature, because of the increase in the quantity and thickness of the interlayer [80]. The surface cleaning, type of the explosive materials and set-up the weld pieces are the prominent parameters controlling the bonding process to reach a high quality joint or clad [81, 82].

2.2.4. Friction welding, friction stir welding and friction spot welding

Aluminum alloys (AA6082 and AA5052) and stainless steel (AISI 304) were welded by friction welding process [7]. It was revealed that the center of the cylindrical bond was the weakest because of the short upset time while the longer upset time originated the intermetallics at the bond interface [83]. An argon atmosphere was used during the friction welding of aluminum alloy to steel, giving stronger interface but the formation of chromium oxide was not fully eliminated by this method [84]. In addition, the formation of $FeAl_3$ as a function of diffusion time was also confirmed [85]. The feasibility of the inertia friction welding of an aluminum alloy (6061-T6) and steel (1018) was studied [86, 87]. The maximum tensile strength of 250 MPa was achieved when the upset pressure was set at 60 MPa although failure was seen to be on the aluminum side after the bonding process and the thickness of the intermetallics (FeAl and Fe_2Al_5) was reported to be about 0.350 μm [88]. Another aluminum alloy (AA1050)

was welded to stainless steel (AISI 304) by rotary friction welding; both in the cylindrical form and fracture through the aluminum side was reported [89]. The alloys grain size also might have an effect on the final properties of the bonds which it was taken into account by Yufeng *et al*. [90].

The characterization of the friction stir welded aluminum alloy (A3003-H112) to stainless steel (304) joints showed that the strength in the center of the bonds and on the advancing side was higher than that at the retreating side [91]. An amorphous layer and oxide films were also observed at the bond interface. In the other investigation, friction stir lap joints of aluminum alloy (AC4C) and zinc-coated steel, which the coupons surfaces was prepared by three different techniques, were studied and it was demonstrated that the AC4C/as received zinc-coated steel joint showed higher fracture strength than the AC4C/brushed finish steel and AC4C/mirror finish steel joints [92]. The other alloy from the aluminum 5××× series (A5083) was friction stir welded to steel (SS400) and it was shown that increasing the rotational speed and pin length causes the reduction in the shear strength of the bonds because of the presence of a thick $FeAl_3$ at the bond interface [93, 94]. It was stated that for the friction spot welding 10 mm pre-hole in the specimen is fine enough to achieve the maximum shear strength of the joint [95]. The significant influence of the pin depth and formation of Al_5Fe_2 and $Al_{13}Fe_4$ was confirmed by the examination of the pure aluminum/low carbon steel bonds prepared by the same solid state welding method [96]. However, Al_4Fe with a hexagonal close-packed structure and a thickness of 0.250 μm was identified when an aluminum ally (6056) was friction stir welded to steel (304) [97].

The other aluminum alloy (5052) and steel (A36) was friction stir-welded and it was shown that increasing the upset pressure to 137.5 MPa and friction time of 0.5 *s* can give a 202 MPa final strength [98]. A German-based research institute (German Aerospace Center-DLR) also patented the friction stir welding of aluminum alloy (A 6056-T4) and stainless steel (304) by an adapted milling machine, but there was no any evidence of the maximum strength of the joints [99]. Aluminum alloy (A5083) has been welded to a mild steel (SS400) by the friction stir welding and a tensile strength was lower than of the aluminum alloy, as a reason of the formation of brittle intermetallics at the upper portion of the bond area [100]. It was correspondingly shown that the counterclockwise rotation of the pin would not lead to the joining of the coupons and

maximum tensile strength can be achieved at the pin offset of 0.2 mm to the steel side. The influence of the annealing, as the post heat treatment process, at 300 °C and 350 °C on the strength of the joints made of steel and aluminum by the friction stir welding was shown that the extended soaking time for the post weld heat treatment lead to the higher strength because of the solution of intermetallics and final size of theses phases, which was around 0.49 μm [101]. The critical thickness of 2.6 μm for the optimum bond strength was reported. To investigate the effect of bonding parameters one study was performed on the joining of pure aluminum and structural steel and the presence of Al3Fe was confirmed as a function of the tool speed [102].

Among the analysis for investigating the friction stir bonded specimens, scanning electron microscopy (SEM) combined with electron backscattered diffraction (EBSD) might be an interesting tool to explore the reactions within the bond area. For instance, in a study after aluminum alloy (AA6181-T4) was friction stir-welded to high-strength steel (DP900) examined and a plastic flow of the material was meticulously studied by EBSD analysis (see Fig.14) [103].

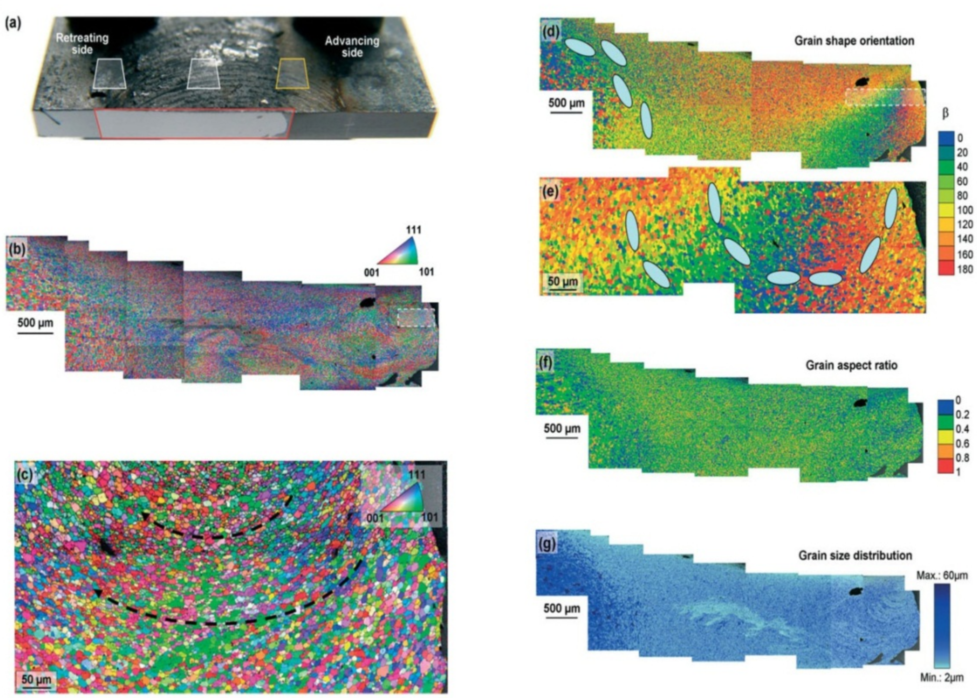

Fig.14. (a) The EBSD analysis locations, (b, and c) orientation of the grains (d, and e) grain shape orientation (f) grain aspect ratio and (g) grain size distribution [103].

One of the important aluminum series which is mostly used in the aerospace industry (7075-T6) has been friction stir welded to mild steel with the tool rotation speed of 400-1200 rpm and the weld travel speed of 100 mm/min [104]. It was observed that the joint strength enhanced by the reduction of the intermetallic thickness. Jiang and Kovecevic [105] exhibited the friction stir welding of a relatively thick aluminum alloy (6061), 6 mm, to a structural steel (AISI 1018) in butt joint configuration and showed that the thickness of $Al_{13}Fe_4$ and Al_5Fe_2 can be controlled. In the continuous work, the offset distance of the tool was considered as the main parameter during the friction stir welding of the relatively thick aluminum alloy and structural steel [106]. The study was focused on the monitoring of the tool wear with acoustic emission sensors (see Fig.15). The presence of $Al_{13}Fe_4$ and Al_5Fe_2 was confirmed in the bond interface and the pin was worn for the rotation speed of 917 rpm and travel distance of 100 mm. Moreover, a designed tool made of Tungsten-Rhenium (W-25%Re) was applied through the study with a pin comprising a triflute with brinks [107].

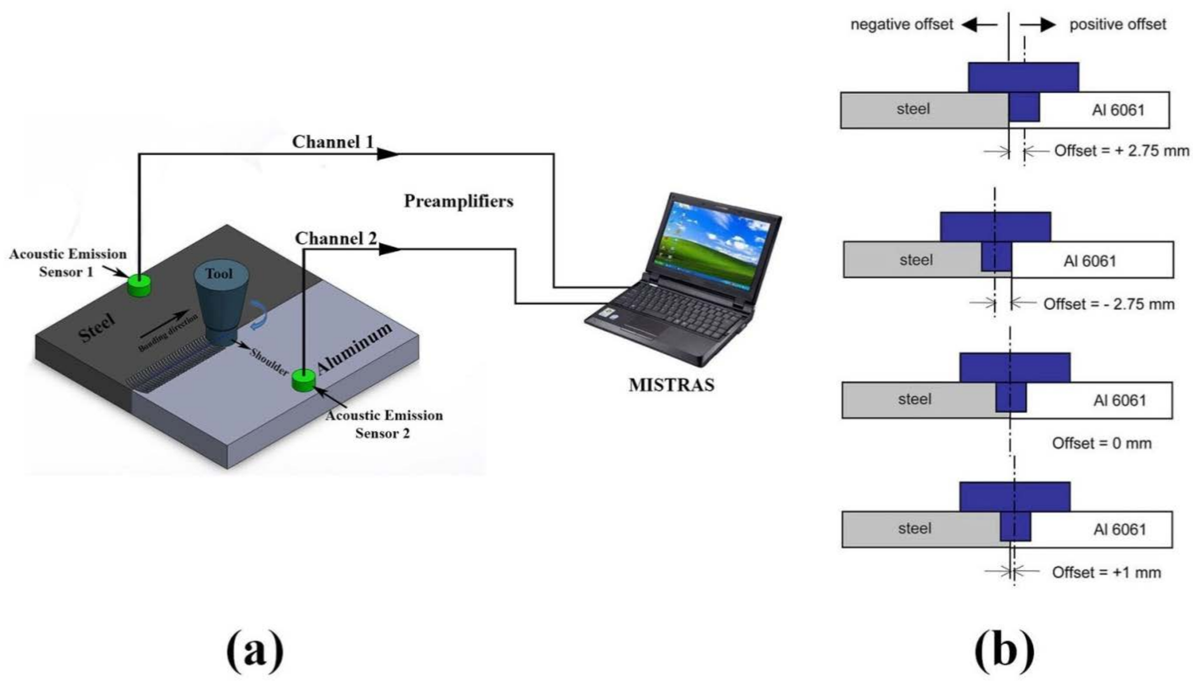

Fig.15. (a) Schematic of the acoustic emission monitoring and (b) location of the probe during the friction stir welding of aluminum alloy (6061) to a structural steel (AISI 1018) [106].

A regular aluminum alloy (A6013-T4) joined to the stainless steel (X5CrNi18-10) by the friction stir welding showed fatigue properties of 30% lower than the aluminum parent alloy [108]. The other type of the aluminum alloy (6016) and high strength steel with different thicknesses were friction spot welded. Different intermetallics ($FeAl_3$, Fe_2Al_5 and $FeAl_2$) were formed, in relation to the pin penetration and rotational velocity (see Fig.16) [109]. The result of the study by Bozzi *et al.* [109] can be confirmed by the outcome of the research work done by Qiu *et al.* [110] where an aluminum alloy (A5052) and a mild steel with a thickness of 1.0 mm were bonded by this method. The other type of the aluminum alloy (5186) was friction stir welded to mild steel and two intermetallics, Al_6Fe and Al_5Fe_2 were observed in the bond area [11].

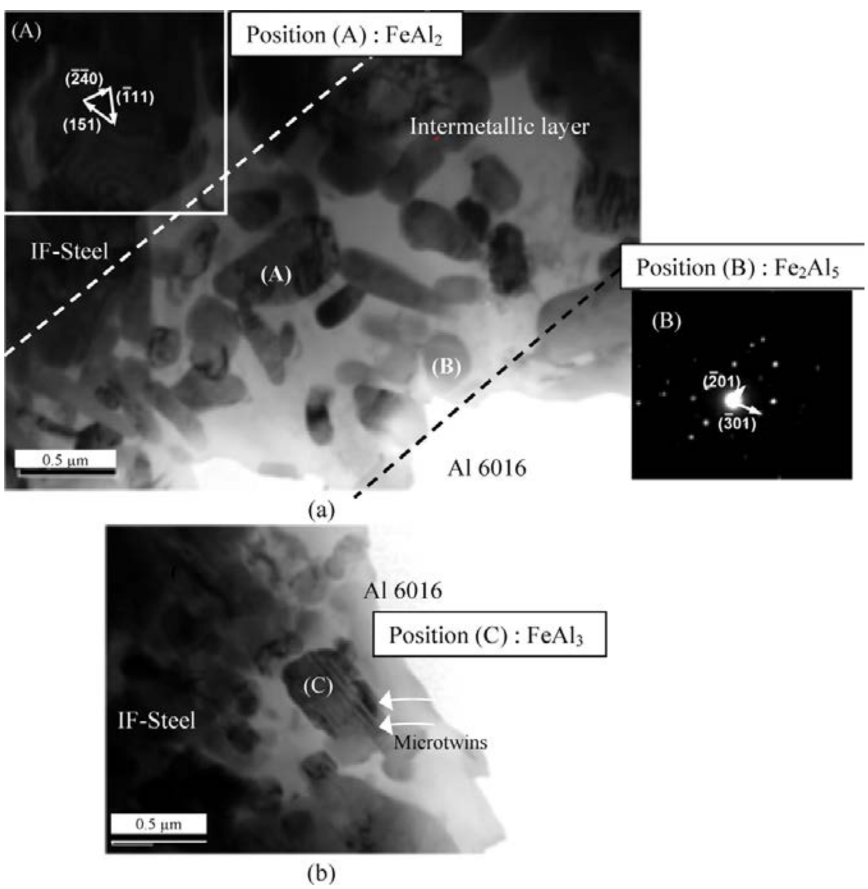

Fig.16. Transmission electron microscope micrographs of the intermetallics (a) diffraction patterns of $FeAl_2$ and Fe_2Al_5 and (b) micrograph of $FeAl_3$ [109].

The thickness of the intermetallics was stated to be a function of dwell time ($X=(Dt)^{0.5}$) as the pin stays in its position for longer time more diffusion time can be given to the alloying elements to move across the bond area [111]. Moreover, a thin aluminum alloy (6061-T6) was friction spot welded to mild steel where a round dent was made on the aluminum side before the bonding but despite the fact that the pre-plasticized area should help to improve the bond quality some unexpected intermetallics like Al_6Fe were formed in the bond zone [112].

2.3. Mixed welding techniques

Gas tungsten arc welding was combined with friction stir welding to join a stainless steel alloy (STS304) to an aluminum alloy (Al6061) achieved a tensile strength of almost 93% of the aluminum alloy, higher than the joints with friction stir welding alone [113]. Laser roll bonding is the other process that benefits from the assistance of the pressure on the top of the bond zone. Laser heating could give higher temperature in a short period of time and its combination with roll bonding of aluminum and steel alloys reported to be non-effective as the significant formation of intermetallics (FeAl, $FeAl_3$, Fe_2Al_5 and Fe_3Al) was detected [5, 114]. In the other assorted method, resistance spot welding and brazing were mixed to join aluminum alloys (6××× series) and low carbon steel where the bonds did not display enough strength as it was required by the industry [115]. The mixed method of gas tungsten arc welding and laser welding was one of the works that demonstrated the heat conduction from the steel side to the aluminum could lead to the partial melting of the aluminum side, resulting in the linear interaction between the alloying elements, presence of complex intermetallics and ultimate strength of 250 MPa [116, 117]. Other combined methods proposed the mixture of the friction stir welding and brazing with the zinc interlayer [118]. The process shows the interaction layer can be controlled by the bonding parameters since the reacted layer thickness of less than 10 μm was reported (Fig.17).

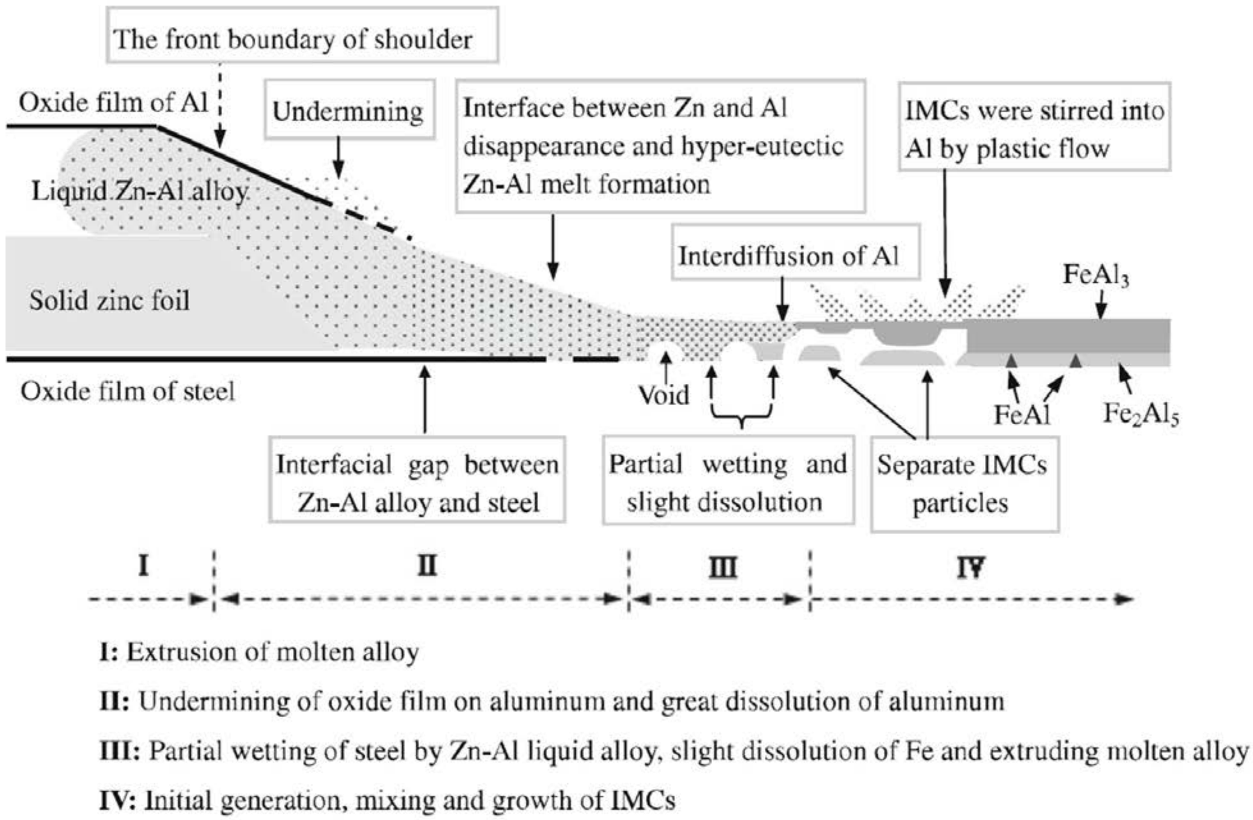

Fig.17. The schematic of the mechanism of the joining in the combined technique of gas tungsten arc welding and brazing [118].

However, there are new novel efforts to combine the welding techniques and quenching systems in the Research Center for the Advanced Manufacturing in the Southern Methodist University which might result in the development of a bonding method to join thin and specifically thick components of the aluminum alloys and advanced steels. The result of the studies will be presented somewhere else with more vision into the details of the mechanical and metallurgical phenomenon elaborated in the bonding processes.

The transitional joint of the aluminum alloys to steels can be achieved if the multi-interlayered transition inserts made of steel and aluminum by solid-state welding processes, especially by explosive welding, is used in order to decrease the level of bonding temperature and heat input to eliminate the formation of the intermetallics. The process then can be extended to the fusion welding like hybrid laser arc welding or friction stir welding of the aluminum alloy

to another aluminum alloy in one side and steel to the other type of the steel in the other side. Therefore, the numerical simulation could provide the optimum welding parameters by satisfying the refinement of the required temperature at the faying surface of the already bonded transition insert metals.

4. Conclusions

The attempt of the present review was to bring the recent works on the joining of the aluminum alloys to the steels into the highlight. There were generally great steps towards the better understanding of the applied welding processes for the joining of the dissimilar materials but for having desirable weldments and materials more efforts have to be put forward. The removal of the intermetallics was a kind of effortless process especially in the fusion welding techniques. The ideal case might be the design of thicker multi-interlayers to completely eliminate the presence of intermetallics in the weldments. More investigations are also needed to find the optimum welding parameters. However, the Al-Fe system is very complex and it still needs serious work for modeling the phase equilibrium under the non-isothermal condition such as the solidification process in the various welding techniques.

Heat generation, fluid flow and plastic flow should be considered while the design of the welding processes has to be perfectly adapted to the alloys. The problem of the intermetallic formation can be solved if the required techniques eliminate the reaction between the iron and aluminum during the heating process. Further analysis, like structural analysis, residual stress analysis, molten pool tracking, phase analysis and the welding physics behind the initiation and extension of the intermetallics is required for the development of the state of the art welding technology. More works on the simulation and modeling of the welding processes are essential to explore the effect of the bonding processes on the microstructure and mechanical properties. Finite element method, finite difference method, phase field modeling and molecular dynamic modeling are examples of the more effective methods to discover the phenomenon involved in the bonding of the aluminum alloys to steel alloys.

5. Acknowledgements

The authors would like to thank Dr. F. Kong for his valuable discussion and ideas in the review of the numerical simulation of the joining process for aluminum and steel alloys. The financial support of the Onodi Tool & Engineering Company is also greatly appreciated.

References

[1] A. Kelkar, R. Roth, J. Clark, Automobile bodies: can aluminum be an economical alternative to steel? , *JOM* (2001) 53 (8) 28-32.

[2] P. F. Mendez, T. W. Eagar, New trends in welding in the aeronautic industry, 2nd Conference of New Manufacturing Trends, Bilboa, Spain (2002) 19-20.

[3] U.R. Kattner, In: binary alloy phase diagrams. ASM International, Materials Park, OH, USA (1990).

[4] L. Agudo, D. Eyidi, C. H. Schmaranzer, E. Arenholz, N. Jank, J. Bruckner, A. R. Pyzalla, Intermetallic Fe_xAl_y-phases in a steel/Al-alloy fusion weld, *Journal of Materials Science* 42 (2007) 4205-4214.

[5] M. J. Rathod and M. Kutsuna, Joining of aluminum alloy 5052 and low-carbon steel by laser roll welding, *Welding Journal* 83 (1) (2004) 16-26.

[6] H. Date, S. Kobayakawa, M. Naka, Microstructure and bonding strength of impact-welded aluminum-stainless steel joints, *Journal of Materials Processing Technology* 85 (1999) 166-170.

[7] R. N. Shubhavardhan, S. Surendran, Friction welding to join stainless steel and aluminum materials, *International Journal of Metallurgical & Materials Science and Engineering (IJMMSE)* 2 (3) (2012) 53-73.

[8] J. Tsujino, K. Hidai, A. Hasegawa, R. Kanai, H. Matsuura, K. Matsushima, T. Ueoka, Ultrasonic butt welding of aluminum, aluminum alloy and stainless steel plate specimens, *Ultrasonics* 40 (2002) 371-374.

[9] P. He, X. Yue, J.H. Zhang, Hot pressing diffusion bonding of a titanium alloy to a stainless steel with an aluminum alloy interlayer, *Materials Science and Engineering A* 486 (2008) 171-176.

[10] M. Acarer, B. Demir, An investigation of mechanical and metallurgical properties of explosive welded aluminum-dual phase steel, *Materials Letters* 62 (2008) 4158-4160.

[11] M. Dehghani, A. Amadeh, S.A.A. Akbari Mousavi, Investigations on the effects of friction stir welding parameters on intermetallic and defect formation in joining aluminum alloy to mild steel, *Materials and Design* 49 (2013) 433-441.

[12] A. Mathieua, S. Pontevicci´, J. Vialab, E. Cicalaa, S. Matti, D. Grevey, Laser brazing of a steel/aluminum assembly with hot filler wire (88% Al, 12% Si), *Materials Science and Engineering A* 435-436 (2006) 19-28.

[13] G. Sierra, P. Peyre, F. Deschaux-Beaumec, D. Stuart, G. Fras, Steel to aluminum key-hole laser welding, *Materials Science and Engineering A* 447 (2007) 197-208.

[14] T. Aizawa, M. Kashani, and K. Okagawa, Application of magnetic pulse welding for aluminum alloys and SPCC steel sheet joints, *Welding Journal*, 86 (2007) 119-124.

[15] M. J. Torkamany, S. Tahamtan, J. Sabbaghzadeh, Dissimilar welding of carbon steel to 5754 aluminum alloy by Nd: YAG pulsed laser, *Materials and Design* 31 (2010) 458-465.

[16] E. Schubert, M. Klassen, I. Zerne, C. Wal, G. Sepold, Light-weight structures produced by laser beam joining for future applications in automobile and aerospace industry, *Journal of Materials Processing Technology* 115 (2001) 2-8.

[17] M. Potesser, T. Schoeberl, H. Antrekowitsch, J. Bruckner, The characterization of the intermetallic Fe-Al layer of steel-aluminum welding, *EPD Congress 2006* Edited by S.M. Howard, R.L. Stephens, C.J. Newman, J.-Y.J. Hwang, A.M. Gokhale, T.T. Chen, TMS (The Minerals, Metals & Materials Society), 2006.

[18] F. Haidara, M.-C. Record, B. Duployer, D. Mangelinck, Phase formation in Al-Fe thin film systems, *Intermetallics* 23 (2012) 143-147.

[19] J. Bruckner, Considering thermal processes for dissimilar metals-joining steel to aluminum in heat-intensive applications, the Fabricator, August 28; 2003, http://www.thefabricator.com/Metallurgy/Metallurgy_Article.cfm?ID=676

[20] W. Gąsior, A. Dębski, Z. Moser, Formation enthalpy of intermetallic phases from Al-Fe system measured with solution calorimetric method, *Intermetallics* 24 (2012) 99-105.

[21] V. T. Witusiewicz, A. A. Bondar, U. Hecht, and T. Y. Velikanova, Phase equilibria in binary and ternary systems with chemical and magnetic ordering, *Journal of Phase Equilibria and Diffusion* (2011) 32:329-349.

[22] H. Zhang, J. Liu, Microstructure characteristics and mechanical property of aluminum alloy/stainless steel lap joints fabricated by MIG welding-brazing process, *Materials Science and Engineering A* 528 (2011) 6179-6185.

[23] H. T. Zhang, J.C. Feng, P. He, H. Hackl, Interfacial microstructure and mechanical properties of aluminium-zinc-coated steel joints made by a modified metal inert gas welding-brazing process, *Materials Characterization* 58 (2007) 588-592.

[24] H. Dong, L. Yang, C. Dong, S. Kou, Arc joining of aluminum alloy to stainless steel with flux-cored Zn-based filler metal, *Materials Science and Engineering A* 527 (2010) 7151-7154.

[25] T. Murakami, K. Nakata, H. Tong, M. Ushio, Dissimilar metal joining of aluminum to steel by MIG arc brazing using flux cored wire, *ISIJ Int*. 43 (10) (2003) 1596-1602.

[26] H. Donga, L. Yanga, C. Dong, S. Kou, Improving arc joining of Al to steel and Al to stainless steel, *Materials Science and Engineering A* 534 (2012) 424-435.

[27] J. L. Song, S. B. Lin, C. L. Yang, G. C. Ma, H. Liu, Spreading behavior and microstructure characteristics of dissimilar metals TIG welding-brazing of aluminum alloy to stainless steel, *Materials Science and Engineering A* 509 (2009) 31-40.

[28] S.B. Lin, J.L. Song, C.L. Yang, C.L. Fan, D.W. Zhang, Brazability of dissimilar metals tungsten inert gas butt welding-brazing between aluminum alloy and stainless steel with Al-Cu filler metal, *Materials and Design* 31 (2010) 2637-2642.

[29] Y. Su, X. Hua, Y. Wu, Effect of input current modes on intermetallic layer and mechanical property of aluminum-steel lap joint obtained by gas metal arc welding, *Materials Science & Engineering A* 578 (2013) 340-345.

[30] R. Cao, G. Yu, J. H. Chen, P. C. Wang, Cold metal transfer joining aluminum alloys-to-galvanized mild steel, *Journal of Materials Processing Technology* 213 (10) (2013) 1753-1763.

[31] R. Qiu, C. Iwamoto, S. Satonaka, The influence of reaction layer on the strength of aluminum/steel joint welded by resistance spot welding, *Materials Characterization* 60 (2009) 156-159.

[32] R. Qiu, C. Iwamoto, S. Satonaka, Interfacial microstructure and strength of steel/aluminum alloy joints welded by resistance spot welding with cover plate, *Journal of Materials Processing Technology* 209 (2009) 4186-4193.

[33] R. Qiu, H. Shi, K. Zhang, Y. Tu, C. Iwamoto, S. Satonaka, Interfacial characterization of joint between mild steel and aluminum alloy welded by resistance spot welding, *Materials Characterization* 61 (2010) 684-688.

[34] R. Qiu, S. Satonaka, C. Iwamoto, Effect of interfacial reaction layer continuity on the tensile strength of resistance spot welded joints between aluminum alloy and steels, *Materials and Design* 30 (2009) 3686-3689.

[35] X. Sun, E.V. Stephens, M. A. Khaleel, H. Shao, M. Kimchi, Resistance spot welding of aluminum alloy to steel with transition material-from process to performance-Part I: Experimental study, 83 (7) *Welding Journal* (2004) 188-195.

[36] X. Sun, M. A. Khaleel, Resistance spot welding of aluminum alloy to steel with transition material-from process to performance-Part II: Finite element analysis of the nugget growth, *Welding Journal* 83 (7) (2004) 197-202.

[37] A. Mathieu, R. Shabadi, A. Deschamps, M. Sueryc, S. MatteÏ, D. Grevey, E. Cicala, Dissimilar material joining using laser (aluminum to steel using zinc-based filler wire), *Optics & Laser Technology* 39 (2007) 652-661.

[38] C. Dharmendra, K.P. Rao, J. Wilden, S. Reich, Study on laser welding–brazing of zinc coated steel to aluminum alloy with a zinc based filler, *Materials Science and Engineering* A 528 (2011) 1497-1503.

[39] M. Alexander, M. Simone, V. Jean-Claude, Laser brazing welding using hot (88%-Aluminum, 12%-Silicon) filler material to join steel with aluminum. In: Laser materials processing conference. Proceeding of ICA- LEO'05, Miami, FL USA, 2005. p. 985-91.

[40] S. Yan, Z. Hong, T. Watanabe, T. Jingguo, CW/PW dual-beam YAG laser welding of steel/aluminum alloy sheets, *Optics and Lasers in Engineering* 48 (2010) 732-736.

[41] S. Meco, G. Pardal, S. Ganguly, R. M. Miranda, L. Quintino, S. Williams, Overlap conduction laser welding of aluminum to steel, *International Journal of Advanced Manufacturing Technology* 6 (2012) DOI 10.1007/s00170-012-4512-6.

[42] K.-J. Lee, S. Kumai and T. Arai, Interfacial microstructure and strength of steel to aluminum alloy lap joints welded by a defocused laser beam, Materials Transactions 46 (8) (2005) 1847-1856.

[43] C. R. Radscheit, Laserstrahlfügen von Aluminium mit Stahl, Ph.D. thesis, BIAS (1996).

[44] R. Shabadi, M. Suery, A. Deschamps, Characterization of joints between aluminum and galvanized steel sheets, *Metallurgical and Materials Characterization A* 44A (2013) 2672-2682.

[45] Y. Kawahito, N. Matsumoto, Y. Abe, S. Katayama, Relationship of laser absorption to keyhole behavior in high power fiber laser welding of stainless steel and aluminum alloy, *Journal of Materials Processing Technology* 211 (2011) 1563-1568.

[46] D.C. Weckman, H.W. Kerr, and J.T. Liu, The effects of process variables on pulsed Nd:YAG laser spot welds: Part II AA 1100 aluminum and comparison to AISI 409 stainless steel, *Metallurgical and Materials Transactions* B 28B (1997) 687-700.

[47] M.J. Zhang, G.Y. Chen, Y. Zhang, K.R. Wu, Research on microstructure and mechanical properties of laser keyhole welding-brazing of automotive galvanized steel to aluminum alloy, *Materials and Design* 45 (2013) 24-30.

[48] H. Laukant, C. Wallmann, M. Müller, M. Korte, B. Stirn, H.-G. Haldenwanger, U. Glatzel, Fluxless laser beam joining of aluminum with zinc coated steel, *Science and Technology of Welding and Joining* 10 (2) (2005) 219-226.

[49] R. Borrisutthekul, T. Yachi, Y. Miyashita, Y. Mutoh, Suppression of intermetallic reaction layer formation by controlling heat flow in dissimilar joining of steel and aluminum alloy, *Materials Science and Engineering A* 467 (2007) 108-113.

[50] N. Cavusoglu, H. Ozden, Automobile manufacturing using laser beam welding, *Welding Journal* (2013) 32-37.

[51] G. Liedl, R. Bielak, J. Ivanova, N. Enzinger, G. Figner, J. Bruckner, H. Pasic, M. Pudar, S. Hamp, Joining of aluminum and steel in car body manufacturing, *Physics Procedia* 12 (2011) 150-156.

[52] Z. B-Gang, C. G.-Qing, Z. C.-guang1, NI. J.-qiang, Structure and mechanical properties of aluminum alloy/Ag interlayer/steel non-centered electron beam welded joints, *Transaction of non-Ferrous Metals Society of China* 21 (2011) 2592-2596.

[53] K.-J. Lee, S. Kumai, T. Arai, T. Aizawa, Interfacial microstructure and strength of steel/aluminum alloy lap joint fabricated by magnetic pressure seam welding, *Materials Science and Engineering A* 471 (2007) 95-101.

[54] S. D. Korea, P. P. Datea, S. V. Kulkarni, Electromagnetic impact welding of aluminum to stainless steel sheets, *Journal of Materials Processing Technology* 208 (2008) 486-493.

[55] M. Soltan Ali Nezhad, A. Haerian Ardakani, A study of joint quality of aluminum and low carbon steel strips by warm rolling, *Materials and Design* 30 (2009) 1103-1109.

[56] H. Danesh Manesh, H. Sh. Shahabi, Effective parameters on bonding strength of roll bonded Al/St/Al multilayer strips, *Journal of Alloys and Compounds* 476 (2009) 292-299.

[57] M. Buchner, B. Buchner, B. Buchmayr, H. Kilian, F. Riemelmoser, Investigation of different parameters on roll bonding quality of aluminum and steel sheets, *International Journal of Material Forming* 1 (1) (2008) 1279-1282.

[58] H. Kawase, M. Makimoto, K. Takagi, Y. Ishida, T. Tanaka, Development of aluminum-clad steel sheet by roll bonding, *Transactions ISIJ* 23 (1983) 628-632.

[59] H. Danesh Manesh, A. Karimi Taheri, Bond strength and formability of an aluminum-clad steel sheet, *Journal of Alloys and Compounds* 361 (2003) 138-143.

[60] P. D. Calderon, D. R. Walmsley, A. Munir, An investigation of diffusion welding of pure and alloyed aluminum to Type 316 stainless steel, *Welding Journal* (1985) 104-112.

[61] L. Peng, L. Yajiang, W. Juan, G. Jishi, Vacuum brazing technology and microstructure near the interface of Al/18-8 stainless steel, *Materials Research Bulletin* 38 (2003) 1493-1499.

[62] M. Roulin, J. W. Luster, G. Karadeniz, A. Mortensen, Strength and structure of furnace-brazed joints between aluminum and stainless steel, *Welding Journal* (1999) 151-155.

[63] W. Deqing, S. Ziyuan and Q. Ruobin, Cladding of stainless steel on aluminum and carbon steel by interlayer diffusion bonding, *Scripta Materialia* 56 (2007) 369-372.

[64] P. Zhang, Y. Du, S. Xing, L. Zhang, D. Zeng, J. Cui, L. Ba, Influence of diffusion time on steel-aluminum solid to liquid bonding interfacial structure, *Journal of Materials Science and Technology* 18 (5) (2002) 468-470.

[65] N. Iwamoto, M. Yoshida, S. Tabata, T. Takeuchi, M. Makino, Diffusion welding of mild steel to aluminum, *Transaction of Japanese Welding Research International* 4(2) 1975) 171-174.

[66] H. Shi, S. Qiao, R. Qiu, X. Zhang, H. Yu, Effect of welding time on the joining phenomena of diffusion welded joint between aluminum alloy and stainless steel, *Materials and Manufacturing Processes* 27 (12) (2012) 1366-1369.

[67] M. K. Karfoul, G. J. Tatlock, R. T. Murray, The behavior of iron and aluminum during the diffusion welding of carbon steel to aluminum, *Journal of Materials Science* 42 (2007) 5692-5699.

[68] M. Mazar Atabaki, N. Wati, J. Idris, Transient liquid phase diffusion brazing of stainless steel 304, *Welding Journal* (2013) 57-63.

[69] M. Mazar Atabaki, N. Wati, J. Idris, Transient liquid phase diffusion bonding of stainless steel 304 using copper and aluminum filler interlayers, *Proceedings of the 26th Heat Treating Society Conference* (ASM International) (2011) 20-43.

[70] S. Kobayashi, T. Yakou, Control of intermetallic compound layers at interface between steel and aluminum by diffusion-treatment, *Materials Science and Engineering A* 338 (2002) 44-53.

[71] F.-C. Yin, M.-X. Zhao, Y.-X. Liu, W. Han, Z. Li, Effect of Si on growth kinetics of intermetallic compounds during reaction between solid iron and molten aluminum, *Transaction of Nonferrous Metals Society China* 23 (2013) 556-561.

[72] H. Springer, A. Kostka, E.J. Payton, D. Raabe, A. Kaysser-Pyzalla, G. Eggeler, On the formation and growth of intermetallic phases during interdiffusion between low carbon steel and aluminum alloys, *Acta Materialia* 59 (2011) 1586-1600.

[73] H. Springer, A. Kostka, J.F. dos Santos, D. Raabe, Influence of intermetallic phases and Kirkendall-porosity on the mechanical properties of joints between steel and aluminum alloys, *Materials Science and Engineering A* 528 (2011) 4630-4642.

[74] M. M. R. Howlader, T. Kaga, T. Sug, Investigation of bonding strength and sealing behavior of aluminum/stainless steel bonded at room temperature, *Vacuum* 84 (2010) 1334-1340.

[75] F. Findik, Recent developments in explosive welding, *Materials and Design* 32 (2011) 1081-1093.

[76] J. H. Han, J. P. Ahn, M. C. Shin, Effect of interlayer thickness on shear deformation behavior of AA5083 aluminum alloy/SS41 steel plates manufactured by explosive welding, *Journal of Materials Science* 38 (2003) 13-18.

[77] Y. Li, H. Hashimoto, E. Sukedai, Y. Zhang, Z. Zhang, Morphology and structure of various phases at the bonding interface of Al/steel formed by explosive welding, *Journal of Electron Microscopy* 49(1) (2000) 5-16.

[78] M. Czechowski, Stress corrosion cracking of explosion welded steel-aluminum joints, *Materials and Corrosion* 55 (6) (2004) 464-467.

[79] R. M. Chao, J. M. Yang, S. R. Lay, Interfacial toughness for the shipboard aluminum/steel structural transition joint, *Marine Structures* 10 (1997) 353-362.

[80] L. Tricarico, R. Spina, D. Sorgente, M. Brandizzi, Effects of heat treatments on mechanical properties of Fe/Al explosion-welded structural transition joints, *Materials and Design* 30 (2009) 2693-2700.

[81] G. A. Young, J. G. Banker, Explosion welded, bi-metallic solutions to dissimilar metal Joining, *Proceedings of the 13th Offshore Symposium* (*Texas Section of the Society of Naval Architects and Marine Engineers*), February 24, 2004, Houston, Texas.

[82] A.A. Akbari Mousavi, S. J. Burley, S. T. S. Al-Hassani, Simulation of explosive welding using the Williamsburg equation of state to model low detonation velocity explosive, *International Journal of Impact Engineering* 31 (2005) 719-734.

[83] S. Fukumoto, H. Tsubakino, K. Okita, M. Aritoshi, T. Tomita, Amorphization by friction welding between 5052 aluminium alloy and 304 stainless steel, *Scripta Materialia* 42 (2000) 807-812.

[84] M. Yılmaz, M. C¸öl, M. Acet, Interface properties of aluminum/steel friction-welded components, *Materials Characterization* 49 (2003) 421-429.

[85] S. Fukumoto S, H. Tsubakino, K. Okita, M. Aritashi, T. Tomita, Friction welding process of 5052 aluminum alloy to 304 stainless steel, *Materials Science Technology* 15 (1999) 1080-1086.

[86] E. Taban, J. E. Gould, J. C. Lippold, Dissimilar friction welding of 6061-T6 aluminum and AISI 1018 steel: Properties and microstructural characterization, *Materials and Design* 31 (2010) 2305-2311.

[87] T. Yokoyama, A. Kogawa, Impact tensile properties of 6061 aluminum alloy to SUS 304 stainless steel friction-welded butt joints, *Welding International* 17 (7) (2003) 514-523.

[88] R. S. Coelho, A. Kostka, J. F. dos Santos, A. R. Pyzalla, Friction-stir dissimilar welding of aluminium alloy to high strength steels: Mechanical properties and their relation to microstructure, *Materials Science & Engineering A* 556 (2012) 175-183.

[89] E. P. Alves, F. P. Neto, C. Y. An, Welding of AA1050 aluminum with AISI 304 stainless steel by rotary friction welding process, *Journal of Aerospace Technology and Management, São José dos Campos*, 2 (3) (2010) 301-306.

[90] S. Yufeng, F. Hidetoshi, T. Yutaka, T. Nobuhiro, N. Kazuhiro, N. Kiyoshi, Microstructure and hardness distribution of friction stir welded 1050 Al and IF steel with different original grain sizes, *Transaction of Japanese Welding Research International* 38 (2) (2009) 43-48.

[91] T. Ogura, Y. Saito, T. Nishida, H. Nishida, T. Yoshida, N. Omichi, M. Fujimoto, A. Hirose, Partitioning evaluation of mechanical properties and the interfacial microstructure in a friction stir welded aluminum alloy/stainless steel lap joint, *Scripta Materialia* 66 (2012) 531-534.

[92] Y.C. Chen, K. Nakata, Effect of the surface state of steel on the microstructure and mechanical properties of dissimilar metal lap joints of aluminum and steel by friction stir welding, *Metallurgical and Materials Transactions A* 39 A (2008) 1985-1992.

[93] K. Kimapong, T. Watanabe, Lap joint of A5083 aluminum alloy and SS400 steel by friction stir welding, *Materials Transactions*, 46 (4) (2005) 835-841.

[94] K. Kimapong, T. Watanabe, Friction stir welding of aluminum alloy to steel, *Welding Journal* (2004) 277-282.

[95] K. Kimapong1, T. Watanabe, Effect of welding process parameters on mechanical property of FSW lap joint between aluminum alloy and steel, *Materials Transactions*, 46(10) (2005) 2211-2217.

[96] A. Elrefaey, M. Gouda, M. Takahashi, and K. Ikeuchi, Characterization of aluminum/steel lap joint by friction stir welding, *Journal of Materials Engineering and Performance* 14 (2005) 10-17.

[97] W.-B. Lee, M. Schmuecker, U. A. Mercardo, G. Biallas, Seung-Boo Jung, Interfacial reaction in steel-aluminum joints made by friction stir welding, *Scripta Materialia* 55 (2006) 355-358.

[98] W.-B. Lee, Y.-M. Yeon, D.-U. Kim, S.-B., Jung, Effect of friction welding parameters on mechanical and metallurgical properties of aluminum alloy 5052-A36 steel joint, *Materials Science Technology* 19 (2003) 773-778.

[99] W. M. Thomas, E. D. Nicholas, J. C. Needham, M. G. Nurch, P. Temple-Smith, C. J. Dawes, Friction stir butt welding. Int Patent App PCT/GB92/02203 and GB Patent App 9125978.8, December 1991, US Patent No. 5,460,317, October 1995.

[100] T. Watanabe, H. Takayama, A. Yanagisawa, Joining of aluminum alloy to steel by friction stir welding, *Journal of Materials Processing Technology* 178 (2006) 342-349.

[101] M. Movahedi, A.H. Kokabi, S.M. Seyed Reihani, W.J. Cheng, C.J. Wang, Effect of annealing treatment on joint strength of aluminum/steel friction stir lap weld, *Materials and Design* 44 (2013) 487-492.

[102] S. Kundu, D. Roy, R. Bhola, D. Bhattacharjee, B. Mishra, S. Chatterjee, Microstructure and tensile strength of friction stir welded joints between interstitial free steel and commercially pure Aluminum, *Materials and Design* 50 (2013) 370-375.

[103] R. S. Coelho, A. Kostka, J. F. dos Santos, Anke R. Pyzalla, EBSD technique visualization of material flow in aluminum to steel friction-stir dissimilar welding, *Advanced Engineering Materials* 10 (2) (2008), 1127- 1133.

[104] T. Tanaka, T. Morishige, T. Hirata, Comprehensive analysis of joint strength for dissimilar friction stir welds of mild steel to aluminum alloys, *Scripta Materialia* 61 (2009) 756-759.

[105] W. H. Jiang, R. Kovacevic, Feasibility study of friction stir welding of 6061-T6 aluminium alloy with AISI 1018 steel, Proc. Instn Mech. Engrs Vol. 218 Part B: *J. Engineering Manufacture* (2004) 1323- 1331.

[106] C.M. Chen, R. Kovacevic, Joining of Al 6061 alloy to AISI 1018 steel by combined effects of fusion and solid state welding, *International Journal of Machine Tools & Manufacture* 44 (2004) 1205-1214.

[107] V. Soundararajan, M. Valant, R. Kovacevic, An overview of R&D work in friction stir welding at SMU, *Metalurjija-Journal of Metallurgy* 12(4) (2006) 275-295.

[108] H. Uzun, C. D. Donne, A. Argagnotto, T. Ghidini, C. Gambaro, Friction stir welding of dissimilar Al 6013-T4 to X5CrNi18-10 stainless steel, *Materials and Design* 26 (2005) 41-46.

[109] S. Bozzi, A. L. Helbert-Etter, T. Baudin, B. Criqui, J.G. Kerbiguet, Intermetallic compounds in Al 6016/IF-steel friction stir spot welds, *Materials Science and Engineering A* 527 (2010) 4505-4509l.

[110] R. Qiu, H. Shi, K. Zhang, Y. Tu, C. Iwamoto, S. Satonaka, Interfacial characterization of joint between mild steel and aluminum alloy welded by resistance spot welding, *Materials Characterization* 61 (2010) 684-688.

[111] M. Watanabe, K. Feng, Y. Nakamura, S. Kumai, Growth manner of intermetallic compound layer produced at welding interface of friction stir spot welded aluminum/steel lap joint, *Materials Transactions* 52 (5) (2011) 953-959.

[112] Y.F. Sun, H. Fujii, N. Takaki, Y. Okitsu, Microstructure and mechanical properties of dissimilar Al alloy/steel joints prepared by a flat spot friction stir welding technique, *Materials and Design* 47 (2013) 350-357.

[113] H. Bang, H. Bang, G. Jeon, I. Oh, C. Ro, Gas tungsten arc welding assisted hybrid friction stir welding of dissimilar materials Al6061-T6 aluminum alloy and STS304 stainless steel, *Materials and Design* 37 (2012) 48-55.

[114] J. Fan, C, Thomy, F. Vollertsen, Effect of thermal cycle on the formation of intermetallic compounds in laser welding of aluminum-steel overlap joints, *Physics Procedia* 12 (2011) 134-141.

[115] C. Y. Choi, D. C. Kim, D. G. Nam, Y. D. Kim, Y. D. Park, A Hybrid joining technology for aluminum/zinc coated steels in vehicles, *Journal of Materials Science and Technology* 26 (9) (2010) 858-864.

[116] G. Sierra, P. Peyre, F. Deschaux Beaume, D. Stuart, G. Fras, Galvanized steel to aluminum joining by laser and GTAW processes, *Materials Characterization* 59 (2008) 1705-1 715.

[117] P. Peyre, G. Sierra, F. Deschaux-Beaume, D. Stuart, G. Fras, Generation of aluminium–steel joints with laser-induced reactive wetting, *Materials Science and Engineering A* 444 (2007) 327-338.

[118] G. Zhang, W. Su, J. Zhang, Z. Wei, Friction stir brazing: a novel process for fabricating Al/steel layered composite and for dissimilar joining of Al to steel, *Metallurgical and Materials Transactions A* 42A (2011) 2850-2861.